ИНСТИТУТ ЯДЕРНОЙ ФИЗИКИ СО АН СССР

V.L.Chernyak, A.R.Zhitnitsky

# ASYMPTOTIC BEHAVIOUR OF EXCLUSIVE PROCESSES IN QCD

4. LEADING TWIST $\pi$ AND $\rho$ MESON WAVE FUNCTIONS AND QCD SUM RULES
5. APPLICATIONS

PREPRINT 83-105

НОВОСИБИРСК

CONTENT



## 4. The leading Twist $\pi$ - and $\rho$ -Meson Wave Functions and the QCD Sum Rules [1.44, 4.2].

As it was pointed out before, the nonperturbative hadron wave functions $\varphi_i(x_j, M \sim 1\ \text{GeV})$ are the fundamental objects of the theory. They determine the distribution of the hadron constituents in the longitudinal momentum fractions $0 \le x_i \le 1$, $\sum x_i = 1$ at $P_z \to \infty$ (the normalization point $M$ determines the maximal virtuality of the constituents).

The main goal of this chapter is to obtain the information about the $\pi$ - and $\rho$ -meson wave functions using the nonperturbative method of the QCD sum rules developed in the papers [1.42]. The wave functions obtained in this way will be used in the following chapters for the calculation of various exclusive amplitudes.

### 4.1. Calculation of the Pion Wave Function Moments

The qualitative description of our approach to the calculation of the wave functions moments, $\langle \xi^n \rangle_{M^2} \equiv \int_{-1}^{1} d\xi\, \xi^n\, \varphi(\xi, M^2)$, has been given in the sect. 1.4 above. Therefore, we start here with corresponding sum rules for the pion wave function $\varphi_\pi^A(\xi)$ (see (1.17)):

$$\frac{1}{\pi M^2}\int_0^\infty ds\, e^{-s/M^2} \operatorname{Im} I_{n0}(s) = \frac{3}{4\pi^2(n+1)(n+3)} + \frac{\langle 0|\frac{\alpha_s}{\pi}G^2|0\rangle}{12M^4} + \frac{16\pi}{81}\left(11+4n\right)\frac{\langle \sqrt{\alpha_s}\bar{u}u\rangle}{M} \quad (4.1)$$

$$\frac{1}{\pi}\operatorname{Im} I_{n0}(s) = f_\pi^2 \langle \xi^n \rangle_\pi \delta(s) + f_A^2 \langle \xi^n \rangle_A \delta(s - m_A^2) + \theta(s - s_n)\frac{3}{4\pi^2(n+1)(n+3)}$$

$$\langle 0|\frac{\alpha_s}{\pi}(G^a_{\mu\nu})^2|0\rangle \simeq 1.2\cdot 10^{-2}\ \text{GeV}^4, \quad \langle 0|\sqrt{\alpha_s}\bar{u}u|0\rangle \simeq -1.35\cdot 10^{-2}\ \text{GeV}$$

We present now some additional qualitative considerations to elucidate further the physical meaning of the sum rules we use. The r.h.s. of the sum rules (4.1) can be rewritten in the

form: $4\pi^2(r.h.s) = \int_{-1-\varepsilon}^{1+\varepsilon} d\zeta\, \zeta^n \tilde{\Psi}(\zeta,M)$, $\varepsilon \to +0$, $\tilde{\Psi}(\zeta,M) = \frac{3}{4}(1-\zeta^2) + \Delta\tilde{\Psi}(\zeta,M)$,

$$\Delta\tilde{\Psi}(\zeta,M) = \frac{1}{2}\left(\delta(1-\zeta) + \delta(1+\zeta)\right)\left[\frac{\pi^2}{3}\left\langle\frac{\alpha_s}{\pi}G^2\right\rangle + \frac{704}{81}\pi^3\frac{\langle\bar{u}u\rangle^2}{M^6}\right] + \frac{1}{2}\left(\delta'(1-\zeta) - \delta'(1+\zeta)\right)\left[\frac{256}{81}\pi^3\frac{\langle\bar{u}u\rangle^2}{M^6}\right], \quad (4.2)$$

i.e. as the $n$-th moment of the "wave function" $\tilde{\Psi}(\zeta,M)$. The first term in $\tilde{\Psi}(\zeta,M)$, which is the perturbation theory contribution (Fig. 4.1), describes the asymptotic wave function $\Psi_{as}(\zeta) = \frac{3}{4}(1-\zeta^2)$. The account of nonperturbative interactions, figs. 4.2 - 4.4, gives the correction $\Delta\tilde{\Psi}(\zeta,M)$. While the asymptotic wave function $\Psi_{as}(\zeta)$ describes the smooth and more or less equal distribution of the total momentum between the two quarks, this is not the case for the "nonperturbative wave function" $\Delta\tilde{\Psi}(\zeta,M)$. The whole momentum is carried here by one quark, while the rest quark is a "wee"*. Therefore, the nonperturbative interaction tends to strengthen or to weaken the role of such configurations in which the total momentum is very unequally distributed between the constituents. The sign of this effect is determined by a relative sign of $\Psi_{as}(\zeta)$ and $\Delta\tilde{\Psi}(\zeta,M)$. If the lower resonance gives a large contribution into the spectral density, then the characteristic distribution of the total momentum between the quarks

---

*) Strictly speaking, the sum rules give information not about the wave functions themselves, but about the numerical values of their moments only. The explicit form of $\Delta\tilde{\Psi}$ depends on the used method of asymptotic expansion in $M^2$. But the qualitative properties discussed, do not depend on this.

will be the same in this state and in the total correlator. If $\Psi_{as}(\zeta)$ and $\Delta\tilde{\Psi}(\zeta,M)$ are of the same sign, then the lowest resonance wave function $\Psi_R(\zeta)$ will be wider than $\Psi_{as}(\zeta)$ (i.e. $\left(\langle\zeta^2\rangle_R\right) > \left(\langle\zeta^2\rangle_{as}\right)$). Just this variant is realized for $\Psi_\pi^A(\zeta)$. If $\Psi_{as}(\zeta)$ and $\Delta\tilde{\Psi}(\zeta,M)$ have opposite signs, $\Psi_R(\zeta)$ will be narrower than $\Psi_{as}(\zeta)$ (i.e. $(\langle\zeta^2\rangle_R) < (\langle\zeta^2\rangle_{as})$). As will be shown below, just this version is realized for the $\rho_L$ meson wave function $\Psi_\rho^T(\zeta)$.* The strength of the effect depends on the relative value of $\Psi_{as}(\zeta)$ and $\Delta\tilde{\Psi}(\zeta,M)$ and is different for different correlators. For instance (see below), the nonperturbative effects are larger for the pion than for the $\rho_L$-meson and so $\Psi_\pi^A(\zeta)$ is wider than $\Psi_\rho^V(\zeta)$.

Let us return now back to the sum rules (4.1) and write their explicit form at $n = 0, 2, 4$:

$$4\pi^2\left(f_\pi^2 + f_A^2 e^{-m_A^2/M^2}\right) + M^2 e^{-s_0/M^2} = M^2\left[1 + \left(\frac{0.2\,\mathrm{GeV}^2}{M^2}\right)^2 + \left(\frac{0.366\,\mathrm{GeV}^2}{M^2}\right)^3\right], \quad (4.3)$$

$$20\pi^2\left(f_\pi^2\langle\zeta^2\rangle_\pi + f_A^2\langle\zeta^2\rangle_A e^{-m_A^2/M^2}\right) + M^2 e^{-s_2/M^2} = M^2\left[1 + \left(\frac{0.45\,\mathrm{GeV}^2}{M^2}\right)^2 + \left(\frac{0.75\,\mathrm{GeV}^2}{M^2}\right)^3\right], \quad (4.4)$$

$$\frac{140}{3}\pi^2\left(f_\pi^2\langle\zeta^4\rangle_\pi + f_A^2\langle\zeta^4\rangle_A e^{-m_A^2/M^2}\right) + M^2 e^{-s_4/M^2} = M^2\left[1 + \left(\frac{0.68\,\mathrm{GeV}^2}{M^2}\right)^2 + \left(\frac{1.12\,\mathrm{GeV}^2}{M^2}\right)^3\right] \quad (4.5)$$

The quantities $s_n$ in (4.3 - (4.5) determine the beginning of the smooth continuum where the spectral density coincides with its asymptotic form.

---

*) Let us apply the operator $\left(\frac{d}{dM^2}M^2\right)$ to (4.1). The pion contribution drops out then and the lowest resonance is now the $A_1$-meson. The relative sign of $\left[\Psi_{as}(\zeta) + \frac{d}{dM^2}M^2\Delta\tilde{\Psi}(\zeta,M)\right]$ is negative and this signals that the $A_1$-meson wave function $\Psi_{A_1}^A(\zeta)$ is narrower than $\Psi_{as}(\zeta)$.

The sum rule (4.3) was first obtained and treated in |1.42|. The value of $f_\pi$ obtained in |1.42| from this sum rule agrees with the experimental one.

The method we use for the treatment of the sum rules is as follows. The scale parameter $M$ in each of the sum rules is varied within such limits that the power corrections at r.h.s. are (5-35)% of the perturbation theory contribution. Because our purpose is to find the values of the "residues" $f_i^2\langle\zeta^n\rangle_i$, we do not try to determine the resonance masses from the sum rules, but take them as known quantities. The residues $f_i^2\langle\zeta^n\rangle_i$ and duality intervals $s_n$ are the fitting parameters and their values are determined from the best fit in each of the sum rules.

The sensitivity of the sum rule to the given resonance contribution can be checked as follows. The quantity $s_n$ varies within $\simeq$ 20% around its optimal value $\bar{s}_n$ obtained from the best fit, and the fits are performed with $s_n$ fixed (within $0.8\,\bar{s}_n \lesssim s_n \lesssim 1.2\,\bar{s}_n$) and the residues $f_i^2\langle\zeta^n\rangle_i$ as the fitting parameters. This variation of $s_n$ imitates the influence of higher perturbative and nonperturbative corrections and other unknown factors. The variation of residues shows then the stability of the results and the sensitivity of the sum rule to the resonance contributions.

The best fit gives for the sum rule (4.3):

$$f_\pi \simeq 131\ \text{MeV},\quad f_{A_1} \simeq (170\text{-}180)\ \text{MeV},\quad \bar{s}_0 \simeq 1.7\ \text{GeV}^2 \qquad (4.6)$$

( $f_{A_1}$ is much more sensitive to the precise value of $s_0$ as compared with $f_\pi$ ). The experimental value of $f_\pi$ is $\simeq$133 MeV, and this agrees well with (4.6).

One can also apply the operator $d/d\left(1/M^2\right)$ to (4.3). The



pion contribution disappears and one can determine $f_{A_1}$ by doing the best fit once again. The result is the same as in (4.6). Besides, one can simply drop out the $A_1$-meson contribution from (4.3) and then the best fit gives: $f_\pi \simeq 129$ MeV, $\bar{s}_0^{(\pi)} \simeq 0.8\ \text{GeV}^2$. Evidently, the value of $s_0^{(\pi)}$ determines now not the beginning of the continuum, but the pion duality interval.

The best fits give for the sum rules (4.4), (4.5):

$$\langle\zeta^2\rangle_\pi\Big|_{\bar{M}^2\simeq 1.5\,\text{GeV}^2} = 0.40,\quad \langle\zeta^2\rangle_A\Big|_{\bar{M}^2=1.5\,\text{GeV}^2} = 0.04\text{-}0.07,\quad \bar{s}_2 = 1.8\,\text{GeV}^2 \qquad (4.7)$$

$$\langle\zeta^4\rangle_\pi\Big|_{\bar{M}^2=2.2\,\text{GeV}^2} = 0.24,\quad \langle\zeta^2\rangle_A = ?\qquad \bar{s}_4 \simeq 2.5\ \text{GeV}^2 \qquad (4.8)$$

The value $\langle\zeta^4\rangle_A$ is small and cann't be determined from the sum rule (4.5), because this sum rule is insensitive to the $A_1$-meson contribution.

Because in the sum rules we have not explicitly introduced the logarithmic corrections due to anomalous dimensions, the values $\langle\zeta^n\rangle$ obtained above are taken at the normalization points corresponding to suitable intermediate values of the scale parameter, $\bar{M}^2$.

It is seen from (4.7) that there is an essential redistribution of contributions in the real spectral density as compared with the asymptotic one. The value of $\langle\zeta^2\rangle_\pi$ is considerably larger and $\langle\zeta^2\rangle_{A_1}$ is considerably smaller than the asymptotic value $\langle\zeta^2\rangle_\pi^{as} = \langle\zeta^2\rangle_{A_1}^{as} = 0.20$, and this agrees with the above presented qualitative considerations.

The questions connected with the accuracy of the results obtained from the sum rule (4.3) (and analogous sum rule for

the $\rho_L$ -meson) have been considered in detail in the original paper [1.42] and the expected accuracy is $\simeq$ 10%. We expect the accuracy $\simeq$ (15-20)% for the results (4.7) and $\simeq$(20-25)% for the results (4.8) (the accuracy decreases as $n$ increases, see below).

We do not consider here the next moments of the wave function * for the following reasons. Because the perturbation theory contribution, fig. 4.1, decreases with $n$, the relative importance of nonperturbative power terms in the sum rules increases (i.e. the expansion parameter at large $n$ is not ($1/M^2$), but ($n/M^2$), see (4.1). This leads to increase of the characteristic values of $\bar{M}_n$ at which the power corrections are, say, $\simeq$ 20% of the perturbation theory contribution. At larger values of the scale parameter $M$ the higher mass resonances and the background contribution play much more important role in the sum rules, while the role of the $\pi$ -meson contribution decreases. Therefore, as $n$ increases the sum rules become less sensitive to the pion contribution.

We do not use also the sum rules for the correlators $I_{22}$, $I_{24}$, $I_{44}$ (in the correlator $I_{nm}$ the first current has $n$ derivatives $(\overleftrightarrow{D})^n$ and the second one $(\overleftrightarrow{D})^m$). The point is that in the correlator $I_{nn}$ intermediate states with spins $0 \le s \le n+1$ also contribute, while in the correlator $I_{no}$ the intermediate states have $s=1$ only, except for the pion being the Goldstone particle. That is why in the sum rules for $I_{nn}$ as compared to that of $I_{no}$ :

a) the background and higher mass states can play a much more important role in the sum rules; b) the role of the pion contribution and the sensitivity of the sum rules to it is smaller. If we ignore the presence of additional resonances with spins $0 \le s \le n+1$ to the correlator $I_{nn}$ (absent in $I_{no}$) and choose the same form for the spectral densities $I_{nn}$ and $I_{no}$, then naturally we obtain in this way larger values of $\langle \xi^n \rangle_\pi$. The reason is that we force the pion by itself to fill a duality interval. Indeed, the value $\langle \xi^2 \rangle_\pi$ obtained in this way from the sum rule $I_{22}$ is: $\langle \xi^2 \rangle_\pi \big|_{\bar{M}^2=1.5\,GeV^2} \simeq 0.45$, and this value does not contradict (4.7) yet. However, the value $\langle \xi^4 \rangle_\pi$ obtained on this way from $I_{44}$ already exceeds the value (4.8) considerably.

We have described the most characteristic properties and the methods for handling the sum rules in detail. Below we do not repeat the reasoning and give only the results.

*) Note only that $\langle \xi^6 \rangle_\pi \big|_{\bar{M}^2=3\,GeV^2} \simeq 0.17$.



## 4.2. The Model Pion Wave Function

In this section we describe the qualitative behaviour of the pion wave function and propose the model for it.

For the reasons which will become more clear later (see, ch.5) we renormalize the above found moment values to the point $M_0 \simeq$ 500 MeV. Using the renormalization group (see ch.3 and appendix B) we obtain:

$$\langle \xi^2 \rangle_{M_0} \simeq 0.46, \quad \langle \xi^4 \rangle_{M_0} \simeq 0.30, \quad M_0 \simeq 500\,MeV. \qquad (4.9)$$

Let us collect now all our knowledge about the pion wave function $\varphi_\pi^A(\xi, M_0) = \varphi_\pi^A(-\xi, M_0)$:

a) $\int_{-1}^{1} d\xi\, \varphi_\pi^A(\xi, M_0) = 1$,

b) $\int_{-1}^{1} d\xi\, \xi^2 \varphi_\pi^A(\xi, M_0) \simeq 0.46$,

c) $\int_{-1}^{1} d\xi\, \xi^4 \varphi_\pi^A(\xi, M_0) \simeq 0.30$.

d) $\varphi_\pi^A(\xi, M_0) \sim (1-\xi^2)$ at $|\xi| \to 1$

(for the last point, see sect. 1.4). Besides, it is reasonable to expect that the ground state (pion) wave function is positive *:

e) $\varphi_\pi^A(\xi, M_0) \geq 0$.

Strictly speaking, all this is insufficient, from mathematical viewpoint, for a reconstruction of the wave function. But in practice this is sufficient, barring the pathological cases. Let us choose the asymptotic wave function $\varphi_{as}(\xi) = \frac{3}{4}(1-\xi^2)$ as a zeroth approximation, fig. 4.5. It is evident that its moment values are too small:

$$\langle \xi^0 \rangle_{as} = 1, \quad \langle \xi^2 \rangle_{as} = 0.20, \quad \langle \xi^4 \rangle_{as} = 0.086,$$

and the realistic pion wave function $\varphi_\pi^A(\xi, M_0)$ is much wider. In what way $\varphi_{as}(\xi)$ should be changed in order to increase essentially the moment values $\langle \xi^2 \rangle$ and $\langle \xi^4 \rangle$ and to keep the overall normalization $\langle \xi^0 \rangle = 1$, the threshold behaviour $\sim (1-\xi^2)$ and the positiveness intact? The simplest possible behaviour of $\varphi_\pi^A(\xi, M_0)$ is shown at fig. 4.5. The most characteristic property of $\varphi_\pi^A(\xi, M_0)$ is the existence of the maxima at $|\xi| \neq 0$ and minimum at $\xi \simeq 0$. (Let us recall in this connection that for the non-relativistic quarks the wave function is : $\varphi_{nonrel}(\xi) = \delta(\xi)$, i.e. each quark

---

*) This property is due to analogy to non-relativistic quantum mechanics, though the mode theorem is lacking, of course, in the QCD.



carries one half of the whole momentum). This means that as a rule a larger part of the pion momentum is carried by one quark.

Based on these considerations, the folloving simple model for the pion wave function is proposed:

$$\varphi_\pi^A(\xi, M_0) = \frac{15}{4}(1-\xi^2)\xi^2, \qquad M_0 \simeq 500\ \text{MeV} \qquad (4.10)$$

The wave function (4.10) has two maxima at $\bar{\xi} \simeq \pm 0.7$ and at these points $\simeq 85\%$ of the pion momentum is carried by one quark and $\simeq 15\%$ by another one. The corresponding values of the moments of this function are :

$$\langle \xi^0 \rangle = 1, \quad \langle \xi^2 \rangle \simeq 0.43, \quad \langle \xi^4 \rangle \simeq 0.24. \qquad (4.11)$$

They agree with the values obtained above from the sum rules (within the existing uncertainities) and exceed considerably the corresponding values for the asymptotic wave function. It is worth noting that the point $M_0 \simeq 500$ MeV is chosen in (4.10) for definiteness alone. The same wave function $\varphi_\pi^A(\xi, M_0) = \frac{15}{4}(1-\xi^2)\xi^2$ can be considered to be normalized, for instance, at the points $M_0 \simeq M_\varrho$ or $M_0 \simeq 1$ GeV equally well, because small variations of the moment values $\langle \xi^2 \rangle_{M_0}$ and $\langle \xi^4 \rangle_{M_0}$ with $M_0$ are smaller than the uncertainties with which they are determined from the sum rules.

Of course, the considerations described above cannot be considered as a strict derivation of the wave function (4.10). We wish to stress however, that the sum rules give very strong limitations (see the points "a" - "d" above) and unambiguously exclude any convex wave function. The model wave function (4.10) which fulfills the sum rules has every reason to repro-

duce correctly all the characteristic properties of the true pion wave function. As will be shown in succeeding chapters, the experimental data on the pionic decay modes of heavy mesons unambiguously exclude convex wave functions which give too small branching ratios, while the wave function (4.10) fits the experimental data well enough.

## 4.3 The $\rho$ -Meson Wave Functions

There are two wave functions of the leading twist 2, $\varphi_\rho^V(z)$ and $\varphi_\rho^T(z)$, for the $\rho_L \equiv \rho_{\lambda=0}$ and $\rho_\perp \equiv \rho_{|\lambda|=1}$ mesons, respectively (see ch.2), and their moments are determined by the following matrix elements:

$$\langle 0|\bar d(z)\gamma_\lambda \exp\{ig\int_{-z}^{z} ds\, v\cdot B(sv)\}u(-z)|\rho_L(q)\rangle_\mu = f_\rho^V q_\lambda \int_{-1}^{1} dz\, e^{iz(zq)}\varphi_\rho^V(z,\mu),$$

$$\langle 0|\bar d(0)\hat z\left(iz\overleftrightarrow{D}\right)^n u(0)|\rho_L(q)\rangle_\mu = f_\rho^V (zq)^{n+1}\langle z^n\rangle_\rho^V, \quad z^2=0, \tag{4.12}$$

$$\langle 0|\bar d(z)\sigma_{\lambda\rho}\exp\{ig\int_{-z}^{z} ds\, v\cdot B(sv)\}u(-z)|\rho_\perp(q)\rangle_\mu = f_\rho^T\left(\varepsilon_\lambda^\perp q_\rho - \varepsilon_\rho^\perp q_\lambda\right)\times$$

$$\int_{-1}^{1} dz\, e^{iz(zp)}\varphi_\rho^T(z,\mu),$$

$$\langle 0|\bar d(0)\sigma_{\lambda\rho}\left(iz\overleftrightarrow{D}\right)^n u(0)|\rho_\perp(q)\rangle_\mu = f_\rho^T\left(\varepsilon_\lambda^\perp q_\rho - \varepsilon_\rho^\perp q_\lambda\right)(zq)^n\langle z^n\rangle_\rho^T; \tag{4.13}$$

$$q_z\to\infty,\ M_\rho \varepsilon_\mu^{\lambda=0}(q)\simeq q_\mu,\ \varepsilon_\mu^\perp = \varepsilon_\mu^{\lambda=\pm1}\sim O(1),\ z^2=0.$$

Here $f_\rho^V \equiv f_\rho$ and $f_\rho^T$ are the dimensional constants which determine the values of the wave functions at the origin and are analogous to $f_\pi$. The value of $f_\rho^V \simeq 200$ MeV is



known experimentally from the $\rho^0 \to e^+e^-$ decay.

Proceeding in similar way to the case of the pion, we use below the sum rules to determine the wave function moments and propose the model wave functions which fulfill the sum rules.

### 4.3.1. The Wave Function of the $\rho_L$ -Meson

The following current is considered:

$$i\int dx e^{iqx}\langle 0|T\, J_n(x)\, j_0^+(0)|0\rangle = (zq)^{n+2} I_n(q^2), \tag{4.14}$$

$$J_n(x) = \bar d(x)\hat z\left(iz\overleftrightarrow{D}\right)^n u(x), \quad z^2=0.$$

The currents in (4.14) are obtained from those in (1.14) by the replacement of $\gamma_\mu\gamma_5 \to \gamma_\mu$. It is clear then that only the fig. 4.3 contribution changes the sign, the rest contributions, figs. 4.1, 4.2, 4.4, are the same as for the pion. Therefore, the sum rules have the form:

$$(f_\rho^V)^2\langle z^n\rangle_\rho^V \exp\left(-\frac{M_\rho^2}{M^2}\right) + \frac{3}{4\pi^2(n+1)(n+3)}M^2\exp\left(-\frac{\bar s_n}{M^2}\right) =$$

$$\frac{3M^2}{4\pi^2(n+1)(n+3)} + \frac{\langle\frac{\alpha_s}{\pi}G^2\rangle}{12M^2} + \frac{16}{81}\pi(4n-7)\frac{\langle\sqrt{\alpha_s}\bar uu\rangle^2}{M^4}. \tag{4.15}$$

Using the fitting procedure described in a previous section, one obtains:

$$f_\rho^V \simeq 194\ \text{MeV}, \qquad \bar s_0 \simeq 1.5\ \text{GeV}^2,$$

$$\langle z^2\rangle_{\bar M^2\simeq 1.2\,\text{GeV}^2} = 0.27, \quad \bar s_2 \simeq 2.6\ \text{GeV}^2, \tag{4.16}$$

$$\langle z^4\rangle_{\bar M^2=1.5\,\text{GeV}^2} = 0.15.$$

The sume rule (4.15) at n=0 was first obtained and treated in /1.42/.

Rescaling the moment values (4.16) to the point $\mu_0$, one obtains:

$$\langle \xi^2 \rangle_\rho^V |_{\mu_0} \simeq 0.29 , \quad \langle \xi^4 \rangle_\rho^V |_{\mu_0} \simeq 0.17 , \quad \mu_0 \simeq 500\,\text{MeV}, \qquad (4.17)$$

In comparison with the corresponding values for the pion:

$$\left.\frac{\langle \xi^2 \rangle_\rho^V}{\langle \xi^2 \rangle_\pi^A}\right|_{\mu_0} \simeq 0.63 , \qquad \left.\frac{\langle \xi^4 \rangle_\rho^V}{\langle \xi^4 \rangle_\pi^A}\right|_{\mu_0} \simeq 0.57 . \qquad (4.18)$$

It is seen that $\varphi_\rho^V(\xi,\mu_0)$ is noticeably narrower than $\varphi_\pi^A(\xi,\mu_0)$, but still wider than $\varphi_{as}(\xi)$, and this agrees with the general qualitative considerations (see the sect.4.1).

We use now the pion wave function (4.10) and the ratios (4.18) to obtain the $\rho_L$- meson model wave function:

$$\varphi_\rho^V(\xi,\mu_0) = \frac{3}{4}(1-\xi^2)\left[1 + 1.5\left(\xi^2 - \frac{1}{5}\right)\right] . \qquad (4.19)$$

For this wave function:

$$\frac{\int_{-1}^{1} d\xi\, \xi^2 \varphi_\rho^V(\xi,\mu_0)}{\int_{-1}^{1} d\xi\, \xi^2 \varphi_\pi^A(\xi,\mu_0)} \simeq \frac{0.27}{0.43} \simeq 0.62 ; \qquad \frac{\int_{-1}^{1} d\xi\, \xi^4 \varphi_\rho^V(\xi,\mu_0)}{\int_{-1}^{1} d\xi\, \xi^4 \varphi_\pi^A(\xi,\mu_0)} \simeq \frac{0.13}{0.24} \simeq 0.55 ,$$

and this agrees with (4.18).

The pion model wave function (4.10) and the $\rho_L$- meson one (4.19) have both the form of a linear combination of two lowest Gegenbauer polinomials:

$$\varphi_{model}(\xi,\mu) = \frac{3}{4}(1-\xi^2)\left[1 + A(\mu)\left(\xi^2 - \frac{1}{5}\right)\right], \qquad (4.19a)$$

$$A(\mu_2) = A(\mu_1)\left[\alpha_s(\mu_2)/\alpha_s(\mu_1)\right]^{50/9\beta_0} , \quad \beta_0 = 11 - \frac{2}{3}n_{fl}.$$

We see that it is sufficient to use this simplest form to describe the main characteristic properties of the wave fucntions. This simple model form (and the corresponding form for the three-particle wave functions) will be widely used below.



The sum of the nonperturbative power corections in (4.15) has the same sign at $n \geq 2$ as the perturbation theory contribution and so tend to increase the moment values (in comparison with $\langle \xi^n \rangle_{as}$ ). But this effect is more mild here than for the pion, because one term at r.h.s. (4.15) has negative sign.

4.3.2. The wave function of the $\rho_\perp$ -meson.

Let us obtain the estimate for the dimensional constant $f_\rho^T$ in (4.13) . Consider with this purpose the correlator

$$i\int dx e^{iqx} \langle 0|T\, \bar{d}(x)\gamma_\mu u(x)\, \bar{u}(0)\sigma_{\nu\lambda} d(0)|0\rangle = (g_{\mu\nu}q_\lambda - g_{\mu\lambda}q_\nu) I(q^2). \qquad (4.20)$$

The perturbation theory contribution is zero in the chiral symmetry limit $m_u = m_d = 0$, and the whole answer is nonzero only due to spontaneous chiral symmetry breaking effects. The diagram shown in fig. 4.6 gives the main contribution at

$$|q^2| \to \infty : \quad I(q^2) = \frac{1}{\pi}\int_0^\infty \frac{ds}{s-q^2} \operatorname{Im} I(s) \to \frac{\langle 0|\bar{u}u + \bar{d}d|0\rangle}{q^2} + O\left(1/q^4\right),$$

$$\frac{1}{\pi}\int_0^\infty ds \operatorname{Im} I(s) = -\langle 0|\bar{u}u + \bar{d}d|0\rangle . \qquad (4.21)$$

As the spectral density falls off rapidly at large $s$ , it seems reasonable to retain only $\rho$ -meson contribution in $\operatorname{Im} I(s)$ :

$$\frac{1}{\pi}\operatorname{Im} I(s) = \left(f_\rho^V M_\rho\right)\left(f_\rho^T\right)\delta(s - M_\rho^2) + \ldots \qquad (4.22)$$

Therefore, one has in this approximation:

$$f_\rho^T \simeq - \frac{\langle 0|\bar{u}u + \bar{d}d|0\rangle}{f_\rho^V M_\rho} \simeq 200\,\text{MeV} \simeq f_\rho^V . \qquad (4.23)$$

We'd like to emphasize that the relation (4.23) obtained from the nondiagonal correlator (4.20) determines not only the absolute value of $f_\rho^\perp$, but its sign as well (i.e. the sign relative to $f_\rho^\parallel$). The fact that $f_\rho^\perp \neq 0$ only due to the spontaneous chiral symmetry breaking is evident beforehand, because in the matrix element $\langle 0|\bar{d}\sigma_{\mu\nu}u|\rho_\perp\rangle$ which determines $f_\rho^\perp$, the operator is not chiral invariant.

We cann't estimate the accuracy of the result (4.23) but the value for $f_\rho^\perp$ obtained below by more accurate method agrees well with (4.23). The values for $f_\rho^\perp$ which are more or less close to (4.23) have also been obtained in [4.3-4.5] by different methods.

Let us obtain now the sum rules for the moments of the wave function $\Psi_\rho^\perp(\zeta)$. Consider for this purpose the correlator:

$$i\int dx e^{iqx}\langle 0|T\, j_\mu^{(n)}(x)\, j_\mu^{+(0)}(0)|0\rangle = 2(zq)^{n+2} I_n(q^2),$$

$$j_\mu^{(n)}(x) = \bar{u}(x)\sigma_{\mu\nu}z_\nu\left(iz\overleftrightarrow{D}\right)^n d(x), \quad z^2=0. \qquad (4.24)$$

The sum rules have the form:

$$\frac{1}{\pi M^2}\int_0^\infty ds\, e^{-s/M^2}\,\mathrm{Im}\, I_n(s) = \frac{3}{4\pi^2(n+1)(n+3)} + \frac{n-1}{n+1}\frac{\langle\frac{ds}{\pi}G^2\rangle}{12M^4} - \frac{64}{81}\pi(n-1)\frac{\langle\sqrt{\alpha_s}\bar{u}u\rangle^2}{M^6},$$

$$\frac{1}{\pi}\mathrm{Im}\, I_n(s) = (f_\rho^\perp)^2\langle\zeta^n\rangle_\rho^\perp\,\delta(s-M_\rho) + (B\text{-meson}) + \theta(s-s_n)\frac{3}{4\pi^2(n+1)(n+3)} \qquad (4.25)$$

Let us point out some specific properties of the sum rules (4.25).

a) There is the $B$-meson contribution and so one should check that not the $B$-meson, but just the $\rho$-meson satu-



rates the sum rules. Using the procedure described in sect.4.1, one can convience himself that the sum rules (4.25) are indeed sensitive to the $\rho$-meson contribution.

b) The contribution of the fig. 4.3 diagram into the sum rules (4.25) equals zero. If the contributions with the quantum numbers $1^{--}$ and $1^{+-}$ are separated out in the spectral density, this is not the case, and the fig. 4.3 contribution gives the vacuum matrix elements of the type $\langle 0|\bar{\Psi}\lambda^a\Psi\cdot\bar{\Psi}\lambda^a\Psi|0\rangle$. Such matrix elements, unlike the earlier considered ones $\langle 0|\bar{\Psi}\gamma_\mu\lambda^a\Psi\cdot\bar{\Psi}\gamma_\mu\lambda^a\Psi|0\rangle$, can have large nonfactoried parts (see, for instance, [4.6]), and this leads to large uncertainities in corresponding sum rules.

c) It is seen from (4.25) that the main power correction $\sim\langle\sqrt{\alpha_s}\bar{u}u\rangle^2$ has at $n\geq 2$ the sign opposite to the perturbation theory contribution. This means (see the sect. 4.1) that the nonperturbative interaction tends to diminish the role of those configurations in which the total momentum is devived unequally between the constituents. Hence, one can expect that the wave function $\Psi_\rho^\perp(\zeta, M\sim 1\,\mathrm{GeV})$ is narrower than $\Psi_{as}(\zeta)$. The quantitative analysis of the sum rules (4.25) confirms this expectation.

The results of the fit are the following:

$$f_\rho^\perp\Big|_{M^2\simeq 0.5\,\mathrm{GeV}^2} \simeq 200\,\mathrm{MeV}. \qquad (4.26)$$

$$\langle\zeta^2\rangle_{M^2\simeq 0.5\,\mathrm{GeV}^2} = 0.14, \quad \bar{s}_2 = 1.5\,\mathrm{GeV}^2, \quad \langle\zeta^4\rangle \approx 0.05.$$

The value of $f_\rho^\perp$ from (4.26) agrees well with (4.23). As it was expected, the wave function $\Psi_\rho^\perp(\zeta, M^2\simeq 0.5\,\mathrm{GeV}^2)$ is narrower than $\Psi_{as}(\zeta)$: $\left(\langle\zeta^2\rangle_\rho^\perp = 0.14\right) < \left(\langle\zeta^2\rangle_{as} = 0.20\right)$. Using the model form (4.19a) and (4.26), one obtains:

$$\varphi_p^T(\zeta, \mu^2=0.5\,\mathrm{GeV}^2)=\frac{15}{16}(1-\zeta^2)(1-\zeta^2),\quad \langle\zeta^2\rangle=0.142,\ \langle\zeta^4\rangle=0.048. \tag{4.27}$$

## 4.4. CONCLUSIONS

On the whole, it has been shown that using the method of the QCD sum rules one is able to find both the dimensional constants $f_i$, which characterize the values of the wave functions at the origin, and the values of the few first wave function moments. This information, being combined with some general properties (the overall normalization, the behaviour at the boundaries,etc.) allows one to reconstruct the main characteristic properties of the wave functions and to write the realistic models for them.

The main qualitative result is that all the considered wave functions differe greatly in their properties both from the nonrelativistic and asymptotic wave functions. They differ greatly also from each other. This difference in their properties results from the different interaction with the nonperturbative vacuum fields in the channels with various quantum numbers. The nonperturbative interactions make the wave functions wider or narrower in comparison with their asymptotic form $\varphi_{as}(\zeta)$. The signs and magnitudes of these nonperturbative effects vary from channel to channel and are, as a rule, sufficiently large.



## 5. APPLICATIONS

The general method for finding the asymptotic behaviour of exclusive amplitudes has been described in chs. 1-3 and the realistic hadronic wave functions have been found in ch.4 above. Therefore, we are now ready to do the concrete calculation of exclusive process probabilities.

Our main assumption in this chapter is that we can restrict ourselves, with reasonable accuracy, to leading terms only and to neglect $\alpha$ power corrections when calculating two-particle decays of charmonium levels (higher twist processes and properties of power corrections are discussed in chs. 8,9). The main difficulty is, of course, due to a small $c$-quark mass, $\bar{M}_c \simeq 1.5$ GeV. It seems at the first sight that the charmonium mass is large enough, $\bar{M}^2 \simeq 10\ \mathrm{GeV}^2$. However, the thing is that the large light meson momenta divide into the smaller quark momenta, and these are the latter that determine the internal momentum transfers and constituent virtualities (sect.3.5). For instance, the mean gluon virtuality in fig. 5.13 is: $\overline{q_{gi}^2} \simeq \bar{x}_i \bar{y}_i M^2$, where $M$ is the charmonium mass, $x_i$ and $y_i$ are the longitudinal momentum fractions carried by two light quarks. The characteristic values of $\bar{x}_i$ and $\bar{y}_i$ are determined by the form of the light meson wave function $\varphi(x)$. If $\varphi(x)$ is sufficiently wide, then $\bar{x}_i, \bar{y}_i \ll 1$ and $\overline{q_{gi}^2} \ll M^2$. If $\overline{q_{gi}^2}$ is too small, then the power corrections will be large and the operator expansion is useless.

We show below in this chapter and in chs. 6, 9, 10 that it is possible to describe a large number of various charmonium decays in an agreement with the experimental data, using

the hadron wave functions $\psi_i(x)$ fulfilling the QCD sum rules. Exclusive decay probabilities are, as a rule, very sensitive to the form of the wave functions $\psi_i(x)$. For instance, the decay probabilities corresponding to the wide and narrow wave functions (both normalized by the condition $\int_{-1}^{1} d\zeta\, \psi_i(\zeta) = 1$) can differ by two orders of magnitude. Therefore, the agreement with the experimental data of a large number of predictions confirms the correctness of the whole approach.

## 5.1. Charmonium decays

The possibility to apply the general method of operator expansions to the description of the heavy quarkonium exclusive decays has been pointed out for the first time in the papers [2.1, 2.3].

We use below the nonrelativistic heavy quarkonium wave functions (see the appendix C).

### 5.1.1. $\chi_0(3415) \to \pi^+\pi^-$

The amplitude has the form, fig. 5.13 [2.3]:

$$M(\chi_c \to \pi^+\pi^-) = (4\pi\alpha_s)^2 \frac{64}{27} f_{\chi_0} \frac{f_\pi^2}{4\bar{M}_c^2} I_{\chi_c} + O(1/\bar{M}_c^4),$$

$$I_{\chi_0} = \int_{-1}^{1} \frac{d\zeta_1 \varphi_\pi^A(\zeta_1)}{1-\zeta_1^2} \int_{-1}^{1} \frac{d\zeta_2 \varphi_\pi^A(\zeta_2)}{1-\zeta_2^2} \frac{1}{1-\zeta_1\zeta_2}\left[1 + \frac{1}{4}\frac{(\zeta_1-\zeta_2)^2}{1-\zeta_1\zeta_2}\right]. \qquad (5.1)$$

Here: $\bar{M}_c$ is the $c$-quark mass, the constant $f_{\chi_0}$ determines the value of the $\chi_0$-wave function at the origin and is analogous to $f_\pi$, $f_\rho$. The decay probability is

$$W(\chi_c \to \pi^+\pi^-) = \frac{1}{32\pi\bar{M}_c} \left| M(\chi_c \to \pi^+\pi^-) \right|^2. \qquad (5.2)$$



According to the Appelquist-Politzer receipe, the total hadronic width of $\chi_0$ is determined by fig. 5.1 diagram and is equal to:

$$W_{tot}(\chi_c \to hadr.) = (4\pi\alpha_s)^2 f_{\chi_0}^2 \frac{1}{4\pi\bar{M}_c^2} \qquad (5.3)$$

Therefore, the partial decay width has the form:

$$Br(\chi_c \to \pi^+\pi^-) = \frac{W(\chi_c \to \pi^+\pi^-)}{W_{tot}(\chi_c \to hadr)} = \left| \pi\bar{\alpha}_s \frac{16\sqrt{2}}{27} \frac{f_\pi}{\bar{M}_c^2} I_{\chi_0} \right|^2. \qquad (5.4)$$

and the constant $f_{\chi_0}$ disappeared*. In (5.4) $\bar{\alpha}_s$ is the effective coupling constant (see below).

We calculate the expression (5.4) as follows [1.44]. In the formula (5.3) we take $\alpha_s$ at the point: $\alpha_s = \alpha_s(M_\chi^2/4) \simeq 0.24$. This point corresponds to the case when each of the two gluons in fig. 5.1 carries one half of the total energy. In formula (5.1) we take $\alpha_s \cdot \alpha_s$ at the points corresponding to the gluon virtualities (fig. 5.13): $\alpha_s(q_1^2) = \alpha_s\left(\frac{1-\zeta_1}{2}\frac{1-\zeta_2}{2}M_\chi^2\right)$ and $\alpha_s(q_2^2) = \alpha_s\left(\frac{1+\zeta_1}{2}\frac{1+\zeta_2}{2}M_\chi^2\right)$. Then we extract them out of the integrals over $\zeta_1$ and $\zeta_2$ replacing $q_{1,2}^2$ by their characteristic values $\bar{q}_1^2$, $\bar{q}_2^2$, the latter being determined by the wave function form. Therefore, $\bar{\alpha}_s$ in (5.4) is: $\bar{\alpha}_s = \left[\alpha_s(\bar{q}_1^2)\,\alpha_s(\bar{q}_2^2)\right] / \alpha_s(M^2/4)$.

In order to show to what extent the wave function form influences the value of the branching ratio (5.4), we take the narrow nonrelativistic wave function: $\varphi_\pi^A(\zeta) = \delta(\zeta)$, which

---

*) Although the Appelquist-Politzer receipe for the total decay widths works up to a factor $\simeq 1.5$-$2$ in some cases, we expect that the accuracy will be better for the ratios like (5.4).

describes the case when each of the two quarks carries one half of the pion momentum. For this wave function: $\alpha_s(\bar{q}_1^2 = M^2/4) = \alpha_s(\bar{q}_2^2 = M^2/4) \simeq 0.24$ , $\bar{\alpha}_s \simeq 0.24$ , and the integral $I_{\chi_0}$ in (5.1) is equal to unity. We have then from (5.4) ( $\bar{M}_c \simeq 1.5$ GeV, $f_\pi \simeq 133$ MeV):

$$Br(\chi_0 \to \pi^+\pi^-) \simeq 2.5 \cdot 10^{-3}\% \,, \quad I_{\chi_0} = 1. \tag{5.5}$$

Analogous calculations with the asymptotic wave function $\varphi_\pi^A(\zeta) = \varphi_{as}(\zeta) = \frac{3}{4}(1-\zeta^2)$ give:

$$Br(\chi_0 \to \pi^+\pi^-) \simeq 3.5 \cdot 10^{-2}\% \,, \quad I_{\chi_0} \simeq 3. \tag{5.6}$$

The experimental value is /2.6/ :

$$Br(\chi_0 \to \pi^+\pi^-) = (0.9 \pm 0.2)\%. \tag{5.7}$$

Therefore, the narrow pion wave function evidently contradicts the experiment.

We use now the model wave function (4.10) which fulfills the QCD sum rules and is much wider: $\varphi_\pi^A(\zeta, \mu_0 \simeq 500\,\text{MeV}) = \frac{15}{4}(1-\zeta^2)\zeta^2$. This wave function has the maxima at the points: $\bar{\zeta} \simeq \pm 0.7$. So the characteristic gluon virtualities in fig. 5.13 are: $\bar{q}_1^2 \simeq \left(\frac{1-\bar{\zeta}_1}{2}\right)\left(\frac{1-\bar{\zeta}_2}{2}\right)M^2 \simeq (500\,\text{MeV})^2$, $\bar{q}_2^2 \simeq \left(\frac{1+\bar{\zeta}_1}{2}\right)\left(\frac{1+\bar{\zeta}_2}{2}\right)M^2 \simeq 9\,\text{GeV}^2$ and correspondingly: $\bar{\alpha}_s \simeq [0.43 \cdot 0.20/0.24] \simeq 0.36$, $(\Lambda \simeq 100\,\text{MeV})$.

As for the characteristic value $\bar{\mu}$ for the $\pi$ -meson wave function normalization point, it is determined mainly by the propagator with the smallest virtualty in fig. 5.13, i.e. $\bar{\mu} \simeq 500$ MeV $\ll$ M ~ 3 GeV . So we can substitute into (5.1) just the wave function at low normalization point, $\varphi_\pi^A(\zeta, \mu_0 \simeq 500\,\text{MeV})$ (4.10).

We have now:



$$Br(\chi_0 \to \pi^+\pi^-) \simeq 1.1\% \,, \quad I_{\chi_0} \simeq 14. \tag{5.8}$$

Evidently, the wider is the wave function $\varphi_\pi^A(\zeta)$ , the larger is the value of the integral $I_{\chi_0}$ . The experimental data (5.7) show clearly that the wave function $\varphi_\pi^A(\zeta, \mu \sim 1\,\text{GeV})$ is much wider than $\varphi_{as}(\zeta)$ , and this agree with the QCD sum rule predictions.

Let us obtain now the prediction for the $\Upsilon$ -family. Because $M_b \simeq 4.75$ GeV, $M_b^2 \simeq 10\,M_c^2 \simeq 22.5\,\text{GeV}^2$, all the charactetistic scales increase by a factor $\simeq 10$. The effective constant $\bar{\alpha}_s$ is now: $\bar{\alpha}_s \simeq [0.25.\ 0.16/0.19] \simeq 0.21$, and the wave function (4.10) is after renormalization: $\varphi_\pi^A(\zeta, \mu^2 \simeq 2.5\,\text{GeV}^2) = \frac{15}{4}(1-\zeta^2)(0.72\zeta^2 + 0.056)$ . As a result:

$$\frac{\Gamma\left({}^3P_0(\bar{b}b)\right)}{\Gamma\left({}^3P_0 \to \text{hadr}\right)} \simeq 2 \cdot 10^{-3}\% \,, \quad I_{\chi_b} \simeq 10.$$

5.1.2. $\chi_2(3555) \to \pi^+\pi^-$.

The expression for the decay amplitude has in this case the form /1.44, 2.4/ :

$$W(\chi_2 \to \pi^+\pi^-) = \frac{1}{240\pi M_c}\left|\left(4\pi\bar{\alpha}_s\right)^2 \frac{32}{27}\frac{f_\pi^2}{4\bar{M}_c^2} f_{\chi_2} I_{\chi_2}\right|^2, \tag{5.9}$$

$$W_{tot}(\chi_2) = \frac{\left(4\pi\bar{\alpha}_s\right)^2 |f_{\chi_2}|^2}{45\pi\,\bar{M}_c}\,; \quad Br(\chi_2 \to \pi^+\pi^-) = \left|\pi\bar{\alpha}_s \frac{8\sqrt{3}}{27}\frac{f_\pi^2}{\bar{M}_c^2} I_{\chi_2}\right|^2, \tag{5.10}$$

$$I_{\chi_2} = \int_{-1}^{1} \frac{d\zeta_1\, \varphi_\pi^A(\zeta_1)}{1-\zeta_1^2} \int_{-1}^{1} \frac{d\zeta_2\, \varphi_\pi^A(\zeta_2)}{1-\zeta_2^2} \frac{1}{1-\zeta_1\zeta_2}\left[1 - \frac{1}{2}\frac{(\zeta_1-\zeta_2)^2}{1-\zeta_1\zeta_2}\right] \tag{5.11}$$

Proceeding as in a previous case, we have/1.44/:

a) $\varphi_\pi^A(\zeta) = \delta(\zeta)$: $Br(\chi_2 \to \pi^+\pi^-) \simeq 10^{-3}\%$, $I_{\chi_2} = 1$;

b) $\varphi_\pi^A(\xi) = \varphi_{as}(\xi) = \frac{3}{4}(1-\xi^2)$:

$$Br(\chi_2 \to \bar\pi^+\bar\pi^-) \simeq 10^{-2}\%\,, \quad I_{\chi_2} \simeq 2.5\,;$$

c) $\varphi_\pi^A(\xi) = \frac{15}{4}(1-\xi^2)\xi^2$:

$$Br(\chi_2 \to \bar\pi^+\bar\pi^-) \simeq 0.24\%\,, \quad I_{\chi_2} \simeq 11. \qquad (5.12)$$

The experimental value is /2.6/ :

$$Br(\chi_2 \to \bar\pi^+\bar\pi^-) = (0.20 \pm 0.11)\%\,. \qquad (5.13)$$

Therefore, this example also shows that the pion wave function at low normalization point is much wider than $\varphi_{as}(\xi)$ . The prediction for the $\Upsilon$ -family is:

$$Br({}^3P_2(\bar b b) \to \bar\pi^+\bar\pi^-) \simeq 0.5\cdot 10^{-3}\%\,.$$

### 5.1.3 $\Psi(3100) \to \bar\pi^+\bar\pi^-$ /1.44/

There is a number of contributions into the decay $\Psi \to \bar\pi^+\bar\pi^-$, see figs 5.2 - 5.4. The main contribution is due to the photon exchange, fig. 5.2, and it can, evidently, be expressed through the pion electromagnetic form factor $F_\pi(Q^2)$ . The contribution of fig. 5.3a includes the additional suppression $\sim \frac{\bar d_s}{\bar u} \simeq 0.1$ due to a loop, as compared with fig. 5.2. The contribution of fig. 5.3b, is zero in the exact isotopic symmetry limit. The nonzero contribution of this diagram is due to $m_d \neq m_u$ , $m_d - m_u \simeq 3\,MeV$ * or due to the antisymmetric in $\xi$ part of the pion wave function $\varphi_\pi^{A(-)}(\xi)$ , which is nonzero due to $SU(2)$ -symmetry breaking effects. In comparison with fig. 5.3a contribution, fig. 5.3b includes the additional factor $\sim\left(\frac{\bar d_s}{\alpha}\langle\xi\rangle\right)$, where: $\bar d_s \simeq 0.3$, $\alpha = \frac{1}{137}$, $\langle\xi\rangle = \langle x_d - x_u\rangle_\pi^A$.

*) This contribution is negligible.



It is shown in ch.6 that: $\langle x_d - x_u\rangle_\pi^A = \int_{-1}^{1} d\xi\,\xi^1\,\varphi_\pi^A(\xi) \simeq \left(\langle 0|\bar u u - \bar d d|0\rangle / \langle 0|\bar u u + \bar d d|0\rangle\right) \simeq 4\cdot 10^{-3}$. Therefore: (fig. 5.3b)/(fig. 5.3a) $\simeq 0.2$, and so the whole contribution of the fig. 5.3 diagrams is $\lesssim 10\%$ of that of fig. 5.2. As for the fig. 5.4 contribution, it includes the 3 -particle pion wave function and is power suppressed ( $\sim 1/M_c^2$ ) in comparison with fig. 5.2. Using the 3 -particle pion wave function $\varphi_{3\pi}$ (see ch.9 ), one can obtain the estimate ( $f_{3\pi} \simeq 0.4\cdot 10^{-2}\,GeV^2$, $(m_u + m_d) \simeq 11\,MeV$ ):

$$\frac{(fig.\,5.4)}{(fig.\,5.2)} \sim \left(f_{3\pi} f_\pi \frac{m_\pi^2}{m_u + m_d} \Big/ f_\pi^2 M_c^2\right) \simeq 2\cdot 10^{-2}.$$

Therefore, our conclusion is that the decay amplitude $\Psi \to \bar\pi^+\bar\pi^-$ is determined by the fig. 5.2 contribution (and so - by the pion form factor $F_\pi$ ) with the accuracy $\simeq \bar d_s/\pi \simeq 10\%$.

We can now write the decay probability in the form:

$$Br_e(\Psi \to \bar\pi^+\bar\pi^-) = \frac{\Gamma(\Psi \to \bar\pi^+\bar\pi^-)}{\Gamma(\Psi \to e^+e^-)} = \frac{1}{4} F_\pi(q^2 = M_\Psi^2), \qquad (5.14)$$

$$-M_\Psi^2 F_\pi(M_\Psi^2) = \frac{32\pi \bar d_s}{9} f_\pi^2 I_\pi^2\,, \quad I_\pi = \int_{-1}^{1} \frac{d\xi}{1-\xi}\,\varphi_\pi^A(\xi). \qquad (5.15)$$

One has for $F_\pi(M_\Psi^2)$ :

a) $\varphi_\pi^A(\xi) = \delta(\xi)$: $\bar d_s = d_s\left(\frac{1-\bar\xi_1}{2}\,\frac{1-\bar\xi_2}{2} M_\Psi^2\right) = d_s(M_\Psi^2/4) \simeq 0.25$, $I_\pi = 1$,
$-M_\Psi^2 F_\pi(M_\Psi^2) \simeq 0.05\,GeV^2$.

b) $\varphi_\pi^A(\xi) = \frac{3}{4}(1-\xi^2)$: $I_\pi = 3/2$, $\bar d_s \simeq 0.35$,
$-M_\Psi^2 F_\pi(M_\Psi^2) \simeq 0.15\,GeV^2$. (5.16)

c) $\varphi_\pi^A(\xi) = \frac{15}{4}(1-\xi^2)\xi^2$: $I_\pi = 2.5$, $\bar d_s \simeq 0.43$,
$-M_\Psi^2 F_\pi(M_\Psi^2) \simeq 0.53\,GeV^2$.

The experimental value of $F_\pi(M_\Psi^2)$ obtained from $\Psi\to\pi^+\pi^-$ decay is |2.6| : $Br(\Psi\to\pi^+\pi^-)=(1.1\pm0.5)\cdot10^{-4}$,

$$\left|M_\Psi^2 F_\pi(M_\Psi^2)\right| = (0.7\pm0.3)\,GeV^2$$

Therefore, the narrow pion wave function contradicts this experiment also.

We have for $\Upsilon\to\pi^+\pi^-$ decay instead of (5.16c):

$$-M_\Upsilon^2 F_\pi(M_\Upsilon^2)\simeq 0.28\,GeV^2,\quad I_\pi\simeq 2.25,$$

$$Br_e(\Upsilon\to\pi^+\pi^-)\simeq 2\cdot10^{-6}.$$

It is seen that in the $\Upsilon$ -region the two-particle decay widths are very small.

### 5.1.4. $\chi_0, \Psi\to\rho_L^+\rho_L^-$; $\chi_2\to\rho_L^+\rho_L^-, \rho_\perp^+\rho_\perp^-$.

Let us remind that according to the selection rules (see ch.2) $\chi_0$ and $\Psi$ decay into the longitudinally polarized $\rho_L=\rho_{\lambda=0}$ mesons only, while $\chi_2$ decays into the transversely polarized $\rho_\perp$ -mesons as well. Evidently, the kinematics for the decays into $\rho_L^+\rho_L^-$ coincides with that into $\pi^+\pi^-$ -decays and so, the formulae (5.4), (5.10) and (5.14) can be used with the replacement $f_\pi\to f_\rho^V$, $\varphi_\pi^A(\zeta)\to\varphi_\rho^V(\zeta)$. Using the $\rho$ -meson wave function (4.19 ) which fulfills the sum rules, we have ( $f_\rho^V\simeq 200$ MeV) |4.2|:

$$\frac{Br(\chi_0\to\rho^+\rho^-)}{Br(\chi_0\to\pi^+\pi^-)}=\left|\frac{(f_\rho^V)^2}{f_\pi^2}\,\frac{I_{\chi_0}(\rho)}{I_{\chi_0}(\pi)}\right|^2\simeq 0.5\simeq\frac{Br(\chi_2\to\rho_L^+\rho_L^-)}{Br(\chi_2\to\pi^+\pi^-)},\quad(5.18)$$

$$\frac{F_\rho(q^2)}{F_\pi(q^2)}=\left(\frac{f_\rho^V}{f_\pi}\,\frac{I_\rho}{I_\pi}\right)^2\simeq 1.\quad(5.19)$$

We predict therefore:

$$Br(\Psi\to\rho^+\rho^-)\simeq 10^{-2}\,\%,\quad(5.20)$$



$$Br(\chi_0\to\rho^+\rho^-)\simeq 0.5\,\%,\quad(5.21)$$

$$Br(\chi_2\to\rho_L^+\rho_L^-)\simeq 0.1\,\%.\quad(5.22)$$

Let us emphasize that if the $\pi$ - and $\rho_L$ -meson wave functions $\varphi_\pi^A(\zeta)$ and $\varphi_\rho^V(\zeta)$ were much alike with each other, one would have instead of (5.18): $Br(\chi_0\to\rho^+\rho^-)/Br(\chi_0\to\pi^+\pi^-)\simeq(f_\rho^V/f_\pi)^4\simeq 5$, and this contradicts the experiment |2.6| *. Really, the QCD sum rules predict that the $\rho_L$ -meson wave function is narrower than the pion one, and this even overcompensates the factor $(f_\rho^V/f_\pi)^4\simeq 5$.

The ratio $Br(\chi_2\to\rho_\perp^+\rho_\perp^-)/Br(\chi_2\to\pi^+\pi^-)$ has the form |2.4, 4.1| :

$$\frac{Br(\chi_2\to\rho_\perp^+\rho_\perp^-)}{Br(\chi_2\to\pi^+\pi^-)}=12\left(\frac{f_\rho^T}{f_\pi}\right)^4\left(\frac{I_{\chi_2}^\perp}{I_{\chi_2}}\right)^2,\quad(5.23)$$

$$I_{\chi_2}^\perp=\int_{-1}^{1}\frac{d\zeta_1\varphi_\rho^T(\zeta_1)}{1-\zeta_1^2}\int_{-1}^{1}\frac{d\zeta_2\,\varphi_\rho^T(\zeta_2)}{1-\zeta_2^2}\,\frac{1}{1-\zeta_1\zeta_2}.$$

Using the wave function of the $\rho_\perp$ -meson $\varphi_\rho^T(\zeta)$ (4.27), which fulfills the sum rules, one has from (5.23) |4.1, 4.2| ($f_\rho^T\simeq 200$ MeV) :

$$\frac{Br(\chi_2\to\rho_\perp^+\rho_\perp^-)}{Br(\chi_2\to\pi^+\pi^-)}\simeq 1.\quad(5.24)$$

Let us point in connection with (5.23) that the coefficient in this ratio is very large: $12(f_\rho^T/f_\pi)^4\simeq 60$ . There-

*) $Br(\chi_0\to\rho^+\rho^-)$ is not measured up to now, but it is known that $Br(\chi_0\to\rho_0\pi^+\pi^-)=(1.7\pm0.6)\,\%$ |2.6| . Besides, it is expected that the $\rho^0\rho^0$ -mode does not dominate the $\rho^0\pi^+\pi^-$ -state |2.5| .

fore, if the $\rho_\perp$ -meson and $\pi$ -wave functions were much alike with each other, than $I^{\perp}_{\chi_2} \simeq I_{\chi_2}$ and one would have: $Br(\chi_2 \to \rho\rho)/Br(\chi_2 \to \pi\pi) \gtrsim 60$ *, i.e. $Br(\chi_2 \to \rho\rho) \gtrsim 12\%$. Although the decay ( $\chi_2 \to \rho\rho$ ) is not measured up to now, such a large branching ratio is, evidently, unrealistic. Therefore, this example shows unambiguously that the $\rho_\perp$-meson wave function $\varphi^{T}_{\rho}(\xi)$ is much more narrow than $\varphi^{A}_{\pi}(\xi)$, and this agrees with the sum rule predictions.

Using the relation (5.22), we have for the total branching ratio |4.2| :

$$\frac{Br(\chi_2 \to \rho^+_\perp \rho^-_\perp + \rho^+_\perp \rho^-_\perp)}{Br(\chi_2 \to \pi^+\pi^-)} \simeq 1.5\,; \quad Br(\chi_2 \to \rho^+\rho^-) \simeq 0.3\% \qquad (5.25)$$

5.1.5. Discussion

Let us discuss here in some detail the questions connected with the accuracy of the formulae obtained above in this section.

a) We use the nonrelativistic wave functions for the heavy quarkonium (see the appendix C) and neglect the binding energy in comparison with the heavy quark mass $\bar{M}_c$ . Although the neglected terms are the power corrections $\lesssim M/\bar{M}_c$ , their effect can be noticeable. For instance, the difference between the mass $M_{\chi_0}$ and $2\bar{M}_c$ is a power corection, but when $2\bar{M}_c$ in (5.4) is replaced by $M_{\chi_0}$ , the answer is changed by a factor $(2\bar{M}_c/M_{\chi_0})^4 \simeq 0.6$ . When calculating explicitly the $\chi_0 \to \pi\pi$ -decay amplitude, it is seen that

*) The contribution of the term $\frac{1}{2}(\xi_1-\xi_2)^2/1-\xi_1\xi_2$ in square brackets in $I_{\chi_2}$ (5.11) is much smaller than the contribution of unity.



there appear both the "current" c -quark mass $M^0_c \simeq 1.25$ GeV and the quarkonium mass $M_{\chi_0}/2 \simeq 1.7$ GeV, and that the effective mass $\bar{M}_c$ entering the answer (5.4) is in the region 1.25 GeV $< \bar{M}_c <$ 1.7 GeV. Our choice $\bar{M}_c \simeq 1.5$ GeV, we expect, accounts mainly for these effects.

b) Our choice of $\bar{\alpha}_s$ is based on the clear physical reasoning. Some small uncertainty arises, however, when we replace $\alpha_s\left(\frac{1+\xi_1}{2}\frac{1+\xi_2}{2}M^2\right)$ by $\alpha_s\left(\frac{1+\bar{\xi}_1}{2}\frac{1+\bar{\xi}_2}{2}M^2\right)$ . Note in connection with this, that the integrals (5.1) and (5.11) have been calculated also with $\alpha_s\left(\frac{1-\xi_1}{2}\frac{1-\xi_2}{2}M^2\right)\alpha_s\left(\frac{1+\xi_1}{2}\frac{1+\xi_2}{2}M^2\right)$ as an integrand factor. The results coincide (with the accuracy $\lesssim 10\%$) with those given in (5.8), (5.12).

c) Because the moment values of the wave functions are determined from the QCD sum rules with uncertainties $\simeq (15-20\%)$, the form of the model wave functions can be varied within these limits. This can give the uncertainty about factor $\simeq 2$ in branching ratios like (5.4), (5.10) (there is also the uncertainty in the wave function mean normalization point $\bar{M}$, but it gives much smaller uncertainty).

d) It is argued in chs. 8,9 that the power corrections constitute $\lesssim 30\%$ in the amplitudes at an overall scale $Q^2 \simeq 10$ GeV$^2$, i.e. there are uncertainties about a factor $\simeq$ (1.5-2) in the ratios like (5.4), (5.10).

On the whole, we can calculate at present the ratios like (5.4), (5.10) with uncertainties within a factor $\simeq 2$. It should be stressed that when wide wave functions are replaced by narrow ones, the results for such ratios change by a factor $\simeq 10^2$.

## 5.2 Gluon Effects in Charmed Meson Weak Decays /1.44/

We describe in this sect. the application of the general methods described above to the calculation of the two-particle decay widths of charmed $D^0$ (1870) and $F^+$(2020)-mesons. It seems that the experimental data available at present /2.6/ cannot be explained within the framework of the standard scheme /5.2, 5.3/. This scheme assumes that the leading contribution gives fig. 5.5 diagram which describes the direct decay of the $C$ -quark. Indeed, the contribution of the annihilation diagram, fig. 5.6 , includes the additional suppression $\sim (m_s/M_D) \simeq 10^{-1}$.

There were a number of suggestions to explain the situation /5.4, 5.5/. The supposition about the strengthening of the annihilation contribution due to one or few gluons emission, fig. 5.7, is the most fruitful, from our viewpoint. The corresponding estimates /5.4, 5.7/ show that the contribution of the fig. 5.7 diagram into the total $D^0$ -meson decay rate may be not small. The exact calculation of fig. 5.7 contribution is not possible at present, however, because the large distance interaction plays an essential role here even in the limit $M_c \to \infty$ , and one needs to know the $u$ -quark wave function inside $D$ -meson, which is unknown. The two-particle exclusive decays are prefereable in this respect, because only fig. 5.8 diagram give the contribution at large $M_c$ in this case. The large distance interaction enters here through the $\pi$ and $K$ -meson wave functions only, and therefore we can reliably estimate these contributions.

It is seen that fig. 5.8 diagram for the $D^0 \to K\pi$ decay is like to fig. 5.13 diagram for $\chi \to \pi\pi$ decay, the main difference is that one hard gluon is replaced by $W$ -boson. Therefore, the method used for the description of charmonium decays can be applied here as well.



We give below the estimate which shows that the annihilation contributions, fig. 5.8 , play an essential role ($\simeq 100\%$) in the two-particle decays of $D^0$ and $F^+$ -mesons. Taking account that the two-particle decays ($K\pi$ , $K^*\pi$ , $K\rho$ ,...) constitute $\simeq 30\%$ of all the $D^0$ -meson decays, one can expect that the total decay rates of $D^0$ and $D^+$ -mesons differ noticeably. Indeed, the available experimental data are /5.8/:

$$\tau(D^+)/\tau(D^0) = \left(2.2 \pm \begin{matrix}0.9\\0.6\end{matrix}\right).$$

Let us present now some estimates. Consider the decay $D^0 \to K^-\pi^+$ . The direct contribution, fig. 5.5, gives the decay amplitude: $M_{direct} \sim G f_\pi M_D^2$ , where $G$ is the Fermi constant, $M_D$ is the $D$ -meson mass. The naive estimate of the annihilation contribution, fig. 5.8, is: $M_{an} \sim G f_\pi f_K f_D C_0$, where the constant $f_D \simeq (160\text{-}175)$ MeV (see ch. 7) characterizes the value of the $D$ -meson wave function at the origin and is analogous with $f_\pi \simeq 133$ MeV and $f_K \simeq 165$ MeV, and $C_0 \sim O(1)$ is a dimensionless constant. Therefore, according to this estimate, $M_{an}/M_{dir} \sim (f_D f_K / M_D^2) C_0 \simeq 10^{-2} C_0 \sim 10^{-2}$, and it seems that the annihilation contribution is negligible. Let us remind in connection with this, that the analogous estimate: $Br(\chi_0 \to \pi^+\pi^-) \sim (f_\pi^2/M_\chi^2)^2 \simeq 10^{-4}\%$ (experimentally $\simeq 1\%$), underestimates the amplitude by two orders. The main loophole of such naive estimates is clear (see sect. 5.1). It is assumed implicitly that the hadronic wave function $\varphi(\xi)$ is like the nonrelativistic wave function $\simeq \delta(\xi)$ and so the corresponding integrals of the wave functions $I(\varphi)$ are $\sim O(1)$. This is not the case, really, and for instance, the integral

$I_{\chi_c}(\varphi_\pi)$ multiplying the ( $\chi_0 \to \pi\pi$ ) amplitude is: $I_{\chi_c} \simeq 14$. The same is true for the $D \to K\pi$ decay. The $\pi$ - and $K$ - meson wave functions are wide enough and the corresponding integrals of them are very large. As a result, the naive estimate $C_0 \sim O(1)$ is wrong and $C_0 \sim 10^2$ really.

Therefore, both the direct and annihilation contributions are of importance in charmed meson decays and interfere with each other. It should be stressed in connection with this that their relative signs can be determined unambiguously for each given decay mode. We show below that in all cases for which the experimental data are available this interference works in the right direction*.

5.2.1 Direct Contributions

Let us consider first the decays of $D$ -meson into two pseudoscalar meson, $D \to PP$ . The weak Hamiltonian has the form /5.9/ :

$$H = \frac{G}{\sqrt{2}}\left[C_1 \bar{s}'\gamma_\mu(1+\gamma_5)c\cdot\bar{u}\gamma_\mu(1+\gamma_5)d' + C_2\,\bar{s}'\gamma_\mu(1+\gamma_5)d'\cdot\bar{u}\gamma_\mu(1+\gamma_5)c\right],$$

$$d' = d\cos\theta + s\sin\theta, \quad s' = s\cos\theta - d\sin\theta, \quad C_{1,2} = \frac{1}{2}(C_+ \pm C_-), \tag{5.26}$$

$$C_- = \left[\frac{\alpha_s(M_c)}{\alpha_s(M_W)}\right]^{4/\beta_0} \simeq 1.48, \quad C_+ = \frac{1}{\sqrt{C_-}} \simeq 0.82, \quad C_1 \simeq 1.15, \quad C_2 \simeq -0.33, \quad \Lambda \simeq 100\,\text{MeV}.$$

We use the factorization of matrix elements when calculating the direct contributions (this is like the approach used in /5.10/ ). As a result, the $D^+ \to \bar{K}^0\pi^+$ decay amplitude has the form:

$$M(D^+ \to \bar{K}^0\pi^+) = -iM_D^2\frac{G}{\sqrt{2}}\cos^2\theta\left[\left(C_1+\tfrac{1}{3}C_2\right)f_+^K f_\pi + \left(C_2+\tfrac{1}{3}C_1\right)f_+^\pi f_K\right], \tag{5.27}$$

$$\langle \bar{K}^0(p_2)|\bar{s}\gamma_\mu c|D^+(p_1)\rangle = f_+^K(p_1+p_2)_\mu + f_-^K(p_1-p_2)_\mu .$$

Below in this section we neglect the $SU(3)$ -symmetry breaking effects. Then:

$$M(D^+ \to \bar{K}^0\pi^+) = -i\frac{G}{\sqrt{2}}\cos^2\theta\, M_D^2 f_+(0) f_\pi \frac{4}{3}(C_1+C_2). \tag{5.28}$$

The dimensionless form factor $f_+(0)$ is unity in the exact $SU(4)$ -symmetry limit. One should expect, therefore, that it can be much smaller really, because the $SU(4)$ -symmetry is badly broken. Using the experimental data /2.6/ : $Br(D^+ \to \bar{K}^0\pi^+) \simeq$ $\simeq 2\%$ and the life time $\tau(D^+) = (6-9)\cdot 10^{-13}$ sec, one has from (5.28):

$$f_+(0) \simeq 0.25 - 0.30. \tag{5.29}$$

5.2.2 Annihilation Contributions

The corresponding diagram is shown in fig. 5.8 (plus three analogous diagrams, fig. 5.8 diagram gives the dominant contribution) and it can be calculated by standard methods. Let us point only that the virtualities of the quark and gluon propagators in fig. 5.8 are $\sim O(M_c^2)$ at large $M_c$ and we neglect the initial $u$ -quark momentum in the $D$ -meson rest frame in comparison with $M_c$ . As a result:

$$M_{ann}(D^0 \to K^-\pi^+) = -i\frac{G}{\sqrt{2}}\cos^2\theta\,\frac{32}{27}\pi\bar{\alpha}_s f_\pi f_K f_D C_1 I_D,$$

$$I_D = I_1 I_2 = \int_{-1}^{1}\frac{d\xi_1\varphi_\pi^A(\xi_1)(1+\xi_1^2)}{(1-\xi_1^2)^2}\int_{-1}^{1}\frac{d\xi_2\varphi_\pi^A(\xi_2)}{1-\xi_2^2}. \tag{5.30}$$

---

*) At $M_c \to \infty$ the annihilation contributions die-off, of course, but at $M_c \simeq 1.5$ GeV they are still important. For the $b$ -quark the annihilation contributions into the amplitudes are $\lesssim 10\%$ of the direct ones.

Subsittuting the pion wave function $\varphi_\pi^A(\zeta)$ (4.10) into $I_1$ and $I_2$ we have: $I_2 = 2.5$, while the integral $I_1$ is logarithmically divergent. With logarithmic accuracy:

$$I_1 \simeq \frac{15}{2}\int_0^{1-\zeta_{max}} \frac{d\zeta}{1-\zeta} = \frac{15}{2}\ln\frac{1}{1-\zeta_{max}} \simeq (8-10), \quad I_D \simeq 20-25.$$

Let us compare also $I_D$ and $I_{x_0}$ (5.1):

$$I = \int_{-1}^{1} \frac{d\zeta_1 \varphi_\pi^A(\zeta_1)}{1-\zeta_1^2} \int_{-1}^{1} \frac{d\zeta_2 \varphi_\pi^A(\zeta_2)}{1-\zeta_2^2} \frac{1}{1-\zeta_1^2\zeta_2^2} \simeq 13,$$

$$I_D = \int_{-1}^{1} \frac{d\zeta_1 \varphi_\pi^A(\zeta_1)}{1-\zeta_1^2} \int_{-1}^{1} \frac{d\zeta_2 \varphi_\pi^A(\zeta_2)}{1-\zeta_2^2} \frac{1+\zeta_1^2}{1-\zeta_1^2} \simeq (1.5-2) I \simeq 20-25.$$

It is seen that $I_D$ is certainly larger than $I$ when the wave function is wide, and the above estimate of $I_D$ is reasonable, from our viewpoint.

Taking expressions (5.28), (5.30) as the characteristic values of the direct and annihilation contributions, we have for their ratio ( $f_{\mathcal{D}} \simeq f_K \simeq$ 165 MeV, see ch.7; $f_+ \simeq 0.3$, see (5.29); $\bar{d}_\zeta \simeq 0.4$, $I_D \simeq$ 20-25):

$$\rho = \frac{M_{ann}}{M_{dir}} = \frac{32}{27}\pi\bar{d}_\zeta \frac{f_D f_K}{M_D^2 f_+(0)} I_D \simeq 0.8-1.0. \qquad (5.31)$$

On the whole, we think that we have given strong enough arguments that $\rho \simeq 1$ (within a factor $\sim 2$ ). This conclusion is one of the main results of this section.

Taking account now in the standard way of the final state interaction* we have (all numbers below are given for $\rho \simeq 1$ ):

---

*) The $K\pi$ -scattering phases $\delta_{1/2}$ and $\delta_{3/2}$ with isospins $I=1/2$ and $I=3/2$ are known in the $D$ -meson region [5.11, 5.12] and are: $\delta_{1/2} \simeq 90^\circ$, $\delta_{3/2} \simeq -30^\circ$ (there is the scalar resonance K(1900) in the vicinity of the $D$ -meson).



$$\frac{\Gamma(D^0 \to \bar{K}^0\pi^0)}{\Gamma(D^0 \to K^-\pi^+)} \simeq 0.7 \qquad \left[0.7^{+0.5}_{-0.3}\right],$$

$$\frac{\Gamma(D^+ \to \bar{K}^0\pi^+)}{\Gamma(D^0 \to K^-\pi^+) + \Gamma(D^0 \to \bar{K}^0\pi^0)} \simeq 0.12 \qquad \left[(0.4\pm0.2)\frac{\tau_{D^0}}{\tau_{D^+}}\right], \qquad (5.32)$$

$$\left(\text{if} \quad \tau_{D^+}/\tau_{D^0} \simeq 2.2 \text{ , then } [0.18 \pm 0.09]\right)$$

where the experimental numbers [2.6] are given in parentheses. The fact that the final state interaction can play the essential role in these decay channels has been pointed out earlier [5.5a]. However, it seems impossible to obtain simultaneously $(\bar{K}^0\pi^0)/(K^-\pi^+) \simeq 1$ and $(\bar{K}^0\pi^+)/(\bar{K}^0\pi^0 + K^-\pi^+) \ll 1$ by the phase choice, if the annihilation amplitude $M_{ann}=0$. (Besides, at $M_{ann}=0$ the ratios are very sensitive to the precise phase values, while in our case the sensitivity is small).

Let us point also that the decay mode $D^0 \to \bar{K}^0\eta'$ is enhanced significantly due to the annihilation contribution. We expect: $(D^0 \to \bar{K}^0\eta')/(D^0 \to K^-\pi^+) \sim 0.5$.

The decays $D \to PV$ into one pseudoscalar and one vector mesons ( $\rho, K^*, \varphi$ ) can be considered in complete analogy. The vector meson has zero helicity in these decays, $M_V \varepsilon_\mu^{\lambda=0}(p) \simeq p_\mu$, and so the kinematics of the $D \to PP$ and $D \to PV$ decays become identical. It seems that the final state interaction is of no importance there, because there is no pseudoscalar resonance in this region. One obtains, in particular:

$$\frac{(D^0 \to \bar{K}^{*0}\pi^0)}{(D^0 \to K^{*-}\pi^+)} \simeq 0.2 \left[0.4^{+0.7}_{-0.2}\right], \quad \frac{(D^0 \to K^{*-}\pi^+)}{(D^0 \to K^-\rho^+)} \simeq 0.7 \left[0.44 \pm 0.2\right] \qquad (5.33)$$

$$\frac{(D^0\to \bar K^0\rho^0)}{(D^0\to K^-\rho^+)}\simeq 0.1\left[0.01^{+0.06}_{-0.01}\right],\quad \frac{(D^+\to \bar K^0\rho^+)}{(D^0\to K^-\rho^+ + \bar K^0\rho^0)}\simeq 0.25. \qquad (5.33)$$

### 5.2.3 Cabibbo-Suppressed Decays of $D$ -Mesons

Let us recall that in this case ( $\sim \sin\theta\cos\theta$ ) the annihilation contributions are present not only in $D^0$ -decays, but in $D^+$ decays also. Consider here $D^+$ decays because the final state interaction is of no importance here. The direct and annihilation contributions have the same signs in $D^+\to \bar K^0K^+$ decay and the annihilation contribution is zero in $D^+\to \pi^+\pi^0$ decay*. One obtains:

$$\frac{(D^+\to \bar K^0K^+)}{(D^+\to \pi^+\pi^0)}\simeq 3.6,\quad \frac{(D^+\to \bar K^0K^+)}{(D^+\to \bar K^0\pi^+)}\simeq 1.8\,tg^2\theta\simeq 0.1\left[0.25\pm 0.15\right] \qquad (5.34)$$

Note also that we do not expect that the $SU(3)$ -symmetry breaking effects lead to a significant invrease of the ratio $(D\to KK)/(D\to\pi\pi)$ . Indeed, the symmetry breaking not only increases $f_\pi\to f_K\simeq 1.25\, f_\pi$ , but changes simultaneously the wave function shape, $\varphi^A_\pi(x)\neq\varphi^A_K(x)$ . It is shown in ch.6 that $\varphi^A_K(x)$ is narrower than $\varphi^A_\pi(x)$, and this tends to compensate the effect due to $f_K>f_\pi$ (see ch.6 for details). We expect therefore that the enhancement of $D\to KK$ , $D\to \bar K^*K$ decays in comparison with those of $D\to\pi\pi$, $D\to\rho\pi$ is mainly due to annihilation contributions.

*) There is the selection rule $\Delta I=1/2$ for annihilation contributions, and $\pi^+\pi^0$ state has $I=2$ .



### 5.2.4 $F^+$ -Meson Decays

The annihilation contributions in $F^+$ -meson decays are proportional to the coefficient $C_2$ and so are $\simeq 3.5$ times smaller compared with the effects due to $C_1$ in $D^0$ -decays (see (5.26), $C_2$ is zero in the absence of QCD logarithmic corrections). We have, in particular, ( $f_F\simeq f_D\simeq 165$ MeV, see ch.7):

$$\Gamma\left(F^+\to\pi^+\eta\right)\simeq 1.2\,\Gamma\left(D^+\to\bar K^0\pi^+\right). \qquad (5.35)$$

It is clear that it is of great interest to measure those decay modes which are highly suppressed in the absence of the annihilation contributions. These are: $D^0\to\bar K^0\eta$, $\bar K^0\eta'$, $\pi^0\eta$, $\pi^0\varphi$, $\bar K^0\omega$; $F^+\to\bar K^0K^+$, $\pi^+\omega$, etc.

On the whole, it has been argued above in this section that the annihilation contributions play an essential role in charmed meson exclusive decays. The account of these contributions leads in many cases to predictions which differ greatly from those of the standard scheme and the results are in all cases in better agreement with the experimental data*.

## 5.3 The Cross-Sections " $\gamma\gamma\to$ Two Mesons"

The role of investigations of the processes "$\gamma\gamma\to$ hadrons" is at present increasing. Interesting experimental information was obtained in the last years at the existing accelerators at DESY and SLAC [5.13] . New prospects will be opened by LEP and by linear electron-positron colliders such as VLEPP at Novosibirsk ( $\sqrt{s}\simeq$ (100-300) GeV) and SLC at Stanford ( $\sqrt{s}\simeq$ (50-70) GeV) [5.14, 5.15] . It has been shown in [5.16] that

*) Further details can be found in [1.44] .

the linear high-energy $e^+e^-$ beams can be converted for these colliders into the $\gamma\gamma$ beams without considerable losses in the energy and the luminosity.

It is clear that the processes with the cross sections which do not decrease with an energy are of importance at high energies. These are the processes with the vacuum quantum numbers in the $t$ -channel. From theoretical point of view, the processes "$\gamma\gamma \to M_1 M_2$" are the simplest nontrivial examples of the cross-sections which can be calculated at present.

There are two types of contributions into the "$\gamma\gamma \to M_1 M_2$" amplitudes: a) the quark exchanges, fig. 5.9, /5.17/ ; b) the gluon exchanges, fig. 5.10, /5.18, 5.19/ . It is well known that the two-particle exchange in the $t$ -channel gives at high energies the contribution into the amplitude $\sim s^{j_1+j_2-1}$, where $j_{1,2}$ are the particle spins. Therefore, the quark exchange contributions, fig. 5.9, give the cross-section decreasing with the energy, $d\sigma/dt \sim s^{-2}$ , while those at fig. 5.10 give $d\sigma/dt \sim s^0$ and dominate at high energies. The virtualities of all the propagators at figs. 5.9 and 5.10 are $\sim O(t)$, and so at $|t| \gg m^2$ the hard kernel of the amplitude can be calculated by using the perturbation theory, while the hadron formation is described in the usual way with the help of hadronic wave functions.

Let us point some characteristic features of the two scattering mechanisms, fig. 5.9 and fig. 5.10.

1. Any meson pair can be produced through the quark exchange mechanism, fig. 5.9: $\pi^{\pm 0}\pi^{\mp 0}$, $\rho_L^{\pm 0}\rho_L^{\mp 0}$, $\rho_\perp^{\pm 0}\rho_\perp^{\mp 0}$ etc., but $\rho^0\varphi$, $\rho^0\psi$, $\omega\phi$. The scattering amplitudes in terms of meson wave functions have been calculated in /5.17/ and have the form:



$$M_i = (4\pi\alpha)(4\pi\bar{\alpha}_s)\frac{f_i^2}{t}\int_{-1}^{1} d\zeta_1 \int_{-1}^{1} d\zeta_2\, \varphi_i(\zeta_1)\varphi_i(\zeta_2) f_i(\zeta_1,\zeta_2,\cos\theta), \quad (5.36)$$

where $\theta$ is the scattering angle, $\varphi_i(\zeta)$ are the meson wave functions, $f_i(\zeta_1,\zeta_2,\cos\theta)$ are the known functions nonsingular at $|\cos\theta| \to 1$ , the explicit form of which can be found in /5.17/ . The dependence of the scattering amplitude (5.36) on $\cos\theta$ through $f_i(\zeta_1,\zeta_2,\cos\theta)$ gives, in principle, the possibility to obtain an information about the properties of the wave functions $\varphi_i(\zeta)$ , by measuring the cross section angular dependence. However, the dependence of the integral in (5.36) on $\cos\theta$ is smooth and so a high accuracy of measurements in a wide region in $\cos\theta$ is required really to obtain a reliable information about the wave function properties. Moreover, the absolute values of the cross sections are very small in this case and it seems it will be very difficult to realize this program.

2. The neutral $C$ -odd mesons can only be produced through the two-gluon exchange mechanism, fig. 5.10: $\rho^0\rho^0$ , $\rho^0\omega$ , $\rho^0\varphi$ $\rho^0\Psi$ , etc. The cross sections of these processes have been calculated in /5.18/ . Let us present here some characteristic numbers for the process "$\gamma\gamma \to \rho^0\rho^0$".

The helicity amplitudes (two photon c.m.s., $\pm$ show the photon helicities, $\rho^0$ -mesons have zero helicities) are:

$$M^{++} = M^{--} \simeq M^{+-} = M^{-+} \simeq i\,\frac{s}{t}\,\frac{f_\rho^2}{t}(4\pi\alpha)\left(4\pi\bar{\alpha}_s\right)^2\frac{1}{\pi}. \quad (5.37)$$

At $s \gg |t| \gg m^2$ :

$$\frac{d\sigma(\gamma\gamma\to\rho^0\rho^0)}{d\sigma(\gamma\gamma\to\mu^+\mu^-)} \simeq 120\pi^2\bar{\alpha}_s^4\,\frac{f_\rho^4}{t^2}\,\frac{s}{|t|} \simeq \begin{cases} 0.1 & \text{at } s = 25\ \text{GeV}^2 \\ 35. & \text{at } s = 10^4\ \text{GeV}^2, \end{cases} \quad (5.38)$$

for $|t| \simeq 2\,GeV^2$, $\bar{\alpha}_s = \alpha_s(t/4) \simeq 0.35$, $f_\rho \simeq 200\,MeV$,

$$\tilde{\sigma}(\rho_L^0\rho_L^0) = \int_{t_{min}} dt \left(\frac{d\sigma}{dt}\right) \simeq \frac{1.25\,nbn}{[t_{min}(GeV)]^3} \simeq 0.15\,nbn \quad \text{at } |t_{min}| \simeq 2\,GeV^2. \tag{5.39}$$

The total cross-section for the light hadron production, fig. 5.12, is /5.20/ :

$$\frac{d\sigma_{tot}}{dt} = \frac{8}{9}\frac{\bar{\alpha}_s^2}{\alpha^2}\left(\frac{16}{9\pi}\alpha^4 \ln^2\frac{|t|}{\mu^2}\right),$$

where

$\mu^2 \simeq \langle k_\perp^2 \rangle \simeq 0.1\,GeV^2$ is the infrared cut off. At $|t_{min}| \simeq 2\,GeV^2$, $\bar{\alpha}_s \simeq 0.3$:

$$\tilde{\sigma}_{tot} = \int_{t_{min}} dt \left(\frac{d\sigma_{tot}}{dt}\right) \simeq 4\,nbn, \quad \frac{\tilde{\sigma}(\rho_L^0\rho_L^0)}{\tilde{\sigma}_{tot}} \simeq 4\%.$$

The two-gluon contributions into $\rho_L^0\rho_L^0$ and $\rho_L^0\varphi_L$ - cross sections are shown in fig. 5.11a ( and denoted as $(\rho_L^0\rho_L^0)_{2gl}$ and $(\rho_L^0\varphi)$ ). Also shown in fig. 5.11a and fig. 5.11b are other two meson production cross-sections which are due to the quark exchange mechanism (this contribution into $\rho_L^0\rho_L^0$ is denoted as $(\rho_L^0\rho_L^0)_{2q}$ ). All curves have been obtained in /5.18/ using the formulae for the cross sections $(\rho_L^0\rho_L^0)_{2gl}$, $(\rho_L^0\varphi_L)_{2gl}$ from /5.18/ and for other cross sections from /5.17/ and the $\pi$, $\rho_L$ and $\rho_\perp$ -wave functions (4.10), (4.19 ) and (4.27). It may be seen from figs. 5.11 that the two gluon contributions exceed considerably the two quark ones at small angles.

Let us point also the following. The above described contributions, figs. 5.9, 5.10 correspond to the hard "point-like part"



of the photon. There are also contributions due to the soft "hadron-like part" of the photon, which are described by the vector dominance model (VDM). In the VDM framework:

$$\frac{d\sigma}{dt}(\gamma\gamma \to \rho^0\rho^0)_{VDM} = const\ \frac{d\sigma}{dt}(\rho^0\rho^0 \to \rho^0\rho^0).$$

However, at large $|t| \gg \mu^2$ :

$$\frac{d\sigma(\rho\rho\to\rho\rho)}{dt} \sim \begin{cases} 1/t^6 & \text{- dimensional counting} \\ 1/t^5 & \text{- Landshoff pinch contribution} \end{cases},$$

while $\left[d\sigma(\gamma\gamma\to\rho^0\rho^0)/dt\right]_{point} \sim 1/t^4$. Therefore, the VDM contributions can be neglected at sufficiently large $|t|$ . They may be noticeable, however, at intermediate values of $|t|$ . Unfortunately, the cross section $\rho^0\rho^0 - \rho^0\rho^0$ at $|t| \gg \mu^2$ is not known at present.

On the whole, the hard parts of various cross sections " $\gamma\gamma \to$ two meson" can at present be calculated reliable enough*. Their properties depend essentially both on the specific features of the QCD perturbation theory and on the meson wave function properties.

## 5.4 The decay $\Psi(3100) \to \pi^0\gamma$

Let us define the decay amplitude as follows:

$$\langle \gamma_\perp(p)\pi^0(p') | S | \Psi(Q)\rangle = i\delta(Q-p-p')\, I\, M_0, \tag{5.40}$$

$$I = e_{\mu\nu\lambda\sigma} p'_\mu \Psi_\nu^\perp p_\lambda \gamma_\sigma^\perp,$$

*) See also /5.21/ , where the cross section $\gamma\gamma \to \bar{P}P$ has been considered.

where $\gamma_\sigma$ and $\Psi_\lambda$ are the photon and $\Psi$ -meson polarization vectors. The contribution of the fig. 5.14 diagram with the photon exchange has the form:

$$eM_\gamma = e(4\pi\alpha)\frac{4\sqrt{2}}{g}\frac{f_\psi f_\pi}{M_\psi^3} I_\pi, \quad I_\pi = \int_{-1}^{1}\frac{d\zeta}{1-\zeta}\varphi_\pi^A(\zeta,\bar{M}), \quad \frac{e^2}{4\pi}=\alpha=\frac{1}{137} \tag{5.41}$$

The characteristic normalization point $\bar{M}$ of the pion wave function is determined here by the virtuality of the quark propagator at fig. 5.14: $\bar{M}^2=(1-\bar{\zeta})M_\psi^2/2 \simeq 0.15\,M_\psi^2 \simeq 1.5\ \mathrm{GeV}^2$. Renormalizing the wave function $\varphi_\pi^A(\zeta,\ M_0\simeq 0.5\ \mathrm{GeV})$ (4.10) to this point, $\varphi_\pi^A(\zeta,\bar{M}^2=1.5\,\mathrm{GeV}^2)=\frac{15}{4}(1-\zeta^2)(0.77\zeta^2+0.046)$, one has: $I_\pi \simeq 2.3$ .

The estimate shows that the total contribution of the two-loop diagrams, fig. 5.15, which describe the small distance contributions, is small*. There are, however, the contributions like those shown in fig. 5.16. They correspond to such a region in the loop integrals for fig. 5.15 diagram, where the quark emitting a photon has a small virtuality. Confining ourselves by the $\rho^0$ -meson contribution, we come, evidently, to the VDM:

$$\langle\gamma_\perp(p)\pi^0(p')|S|\Psi(Q)\rangle_{VDM} = -e\frac{f_\rho}{M_\rho\sqrt{2}}\gamma_\mu^\perp\langle\rho_\mu^\perp(p)\pi^0(p')|S|\Psi(Q)\rangle, \tag{5.42}$$

$$\langle\rho_\mu^\perp(p)\pi^0(p')|S|\Psi(Q)\rangle = i\delta(Q-p-p')I_\mu M_3,$$

$$I_\mu = e_{\alpha\beta\lambda\mu}p'_\alpha\Psi_\beta p_\lambda .$$

---

*) This two-loop contribution doesn't contain any large logarithm $\sim \ln M_\psi^2/\mu^2$ , because the corresponding one loop and the Born diagrams are equal zero.



Therefore, the total decay amplitude $M_0$ has the form:

$$M_0 = e\left(M_\gamma - \frac{f_\rho}{M_\rho\sqrt{2}}M_3\right). \tag{5.43}$$

The amplitude $M_3$ of the $\Psi\to\rho\pi$ decay is calculated in sect. 9.1 (see (9.5) and below), and the relative sign of $M_3$ and $M_\gamma$ is determined unambiguously: $(M_3/M_\gamma)<0$.

Therefore, the photon exchange and the VDM contributions add to each other in (5.43).

The $\Psi\to e^+e^-$ decay width is:

$$\Gamma(\Psi\to e^+e^-)=\frac{(4\pi\alpha)^2}{27\pi}\frac{|f_\psi|^2}{M_\psi}; \qquad Br\left(\frac{\Psi\to e^+e^-}{\Psi\to all}\right)\simeq 7.5\%\ /2.6/ \tag{5.44}$$

Using (5.41) with $I_\pi\simeq 2.3$ , we can now represent $Br(\Psi\to\pi^0\gamma)/(\Psi\to e^+e^-)$ in the form:

$$Br\left(\frac{\Psi\to\pi^0\gamma}{\Psi\to e^+e^-}\right)=\left|+\left(\frac{Br(\Psi\to\rho^0\pi^0)}{Br(\Psi\to e^+e^-)}\right)^{1/2}\frac{|e|f_\rho}{M_\rho\sqrt{2}}+1\cdot10^{-2}\right|^2 = \tag{5.45}$$

$$\left|+\left(\frac{0.4\%}{7.5\%}\right)^{1/2}\frac{|e|f_\rho}{M_\rho\sqrt{2}}\cdot10^2+1.\right|^2\cdot10^{-4}\simeq(1.3+1.0)^2\cdot10^{-4}\simeq 5.3\cdot10^{-4}.$$

The amplitude $M_3$ is calculated in sect. 9.1, but in order to obtain more accurate number we substituted into (5.45) the experimental value of $Br(\Psi\to\rho^0\pi^0)$ /2.6/. We have finally from (5.45), (5.44):

$$Br\left(\frac{\Psi\to\pi^0\gamma}{\Psi\to all}\right)\simeq 4\cdot10^{-5}. \tag{5.46}$$

The experimental value is /5.22/:

$$Br\left(\frac{\Psi\to\pi^0\gamma}{\Psi\to all}\right)=(3.6\pm1.1\pm0.8)\cdot10^{-5},$$

so that the agreement is good.

Let us emphasize that the inferference of the two contributions in (5.45) is of crucial importance, and the theory predicts both the magnitudes of these contributions and their relative sign. The opposite relative sign contradicts the expriement.

## 5.5 CONCLUSIONS

It has been shown above in this chapter that it is possible to obtain a large number of predictions for various exclusive processes - the strong, electromagnetic and weak decays of heavy mesons, the form factors, etc., in agreement with the available experimental data. Besides, it was demonstrated that both the nonrelativistic and the asymptotic forms of meson wave functions contradict the experiment, while the wave functions obtained with the help of the QCD sum rules lead to an agreement with the experiment. We want to emphasize once more that the absolute values of the exclusive process probabilities are, as a rule, very sensitive to the precise form of hadronic wave functions. Varying the form of the wave functions considerably, but keeping the normalization intact, $\int_{-1}^{1} d\xi\, \varphi_i(\xi) = 1$, we can get the probabilities changing within two orders of a magnitude.

The sum rules predict that some wave functions $\left(\varphi_\rho^T(\xi)\dots\right)$ are narrower while the other ones $\left(\varphi_\pi^A(\xi)\dots\right)$ are much wider in comparison with the asymptotic wave function, and this agrees with the experiment, while the opposite case clearly contradicts the experiment.

The large number of confirmed predictions can hardly be a mere coincidence, but shows that the theory works really in the charm region. We know no other approach which allows one to describe simultaneously all the processes considered above.



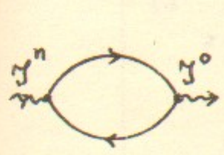


fig. 4.1

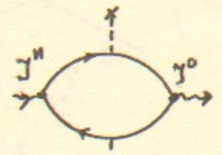


fig. 4.2

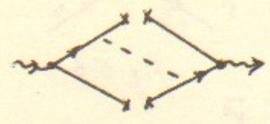

fig. 4.3

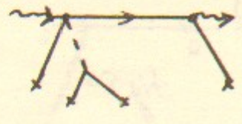

fig. 4.4

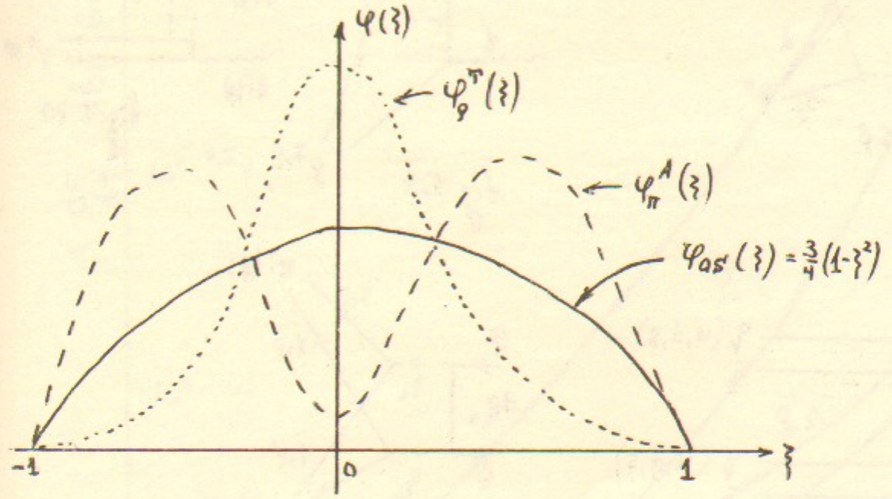


fig. 4.5

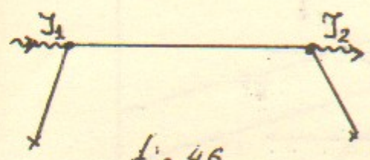


fig. 4.6

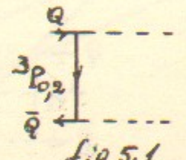


fig. 5.1

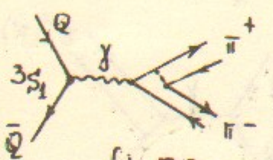


fig. 5.2

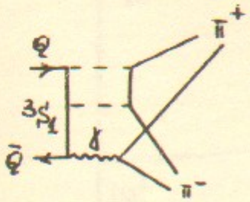


fig. 5.3a

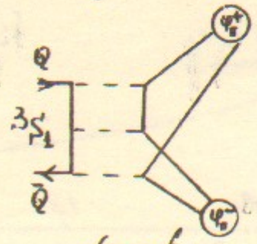


fig. 5.3b

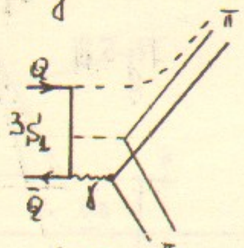


fig. 5.4

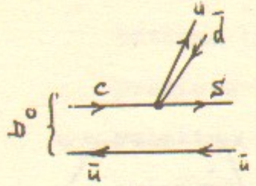


fig. 5.5

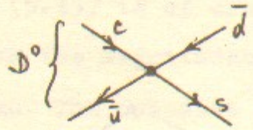


fig. 5.6

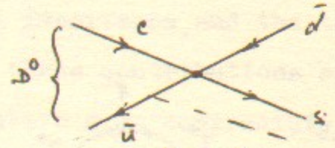


fig. 5.7

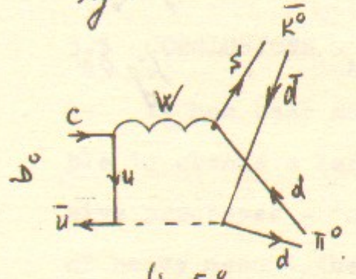


fig. 5.8

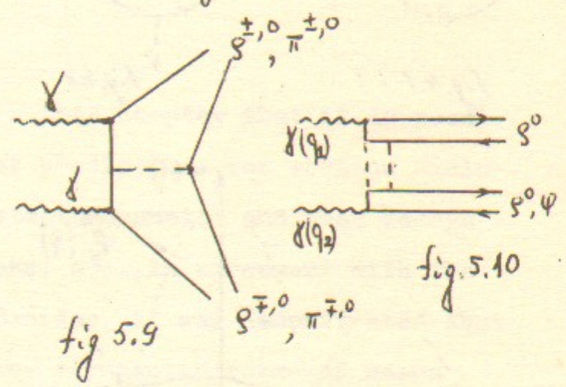


fig 5.9

fig. 5.10

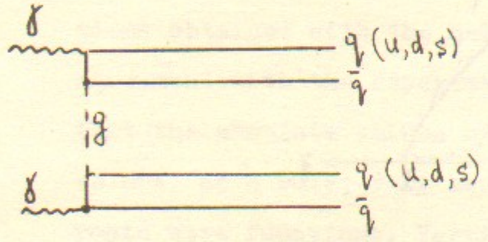


fig. 5.12

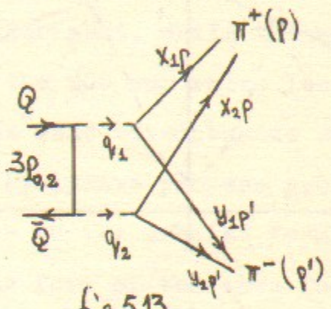


fig 5.13

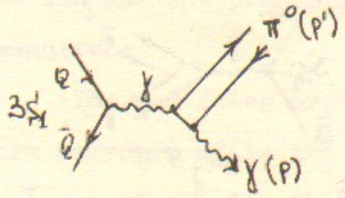


fig 5.14

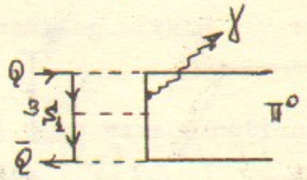


fig. 5.15

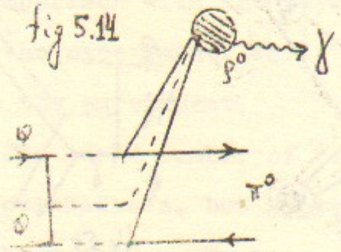


fig. 5.16



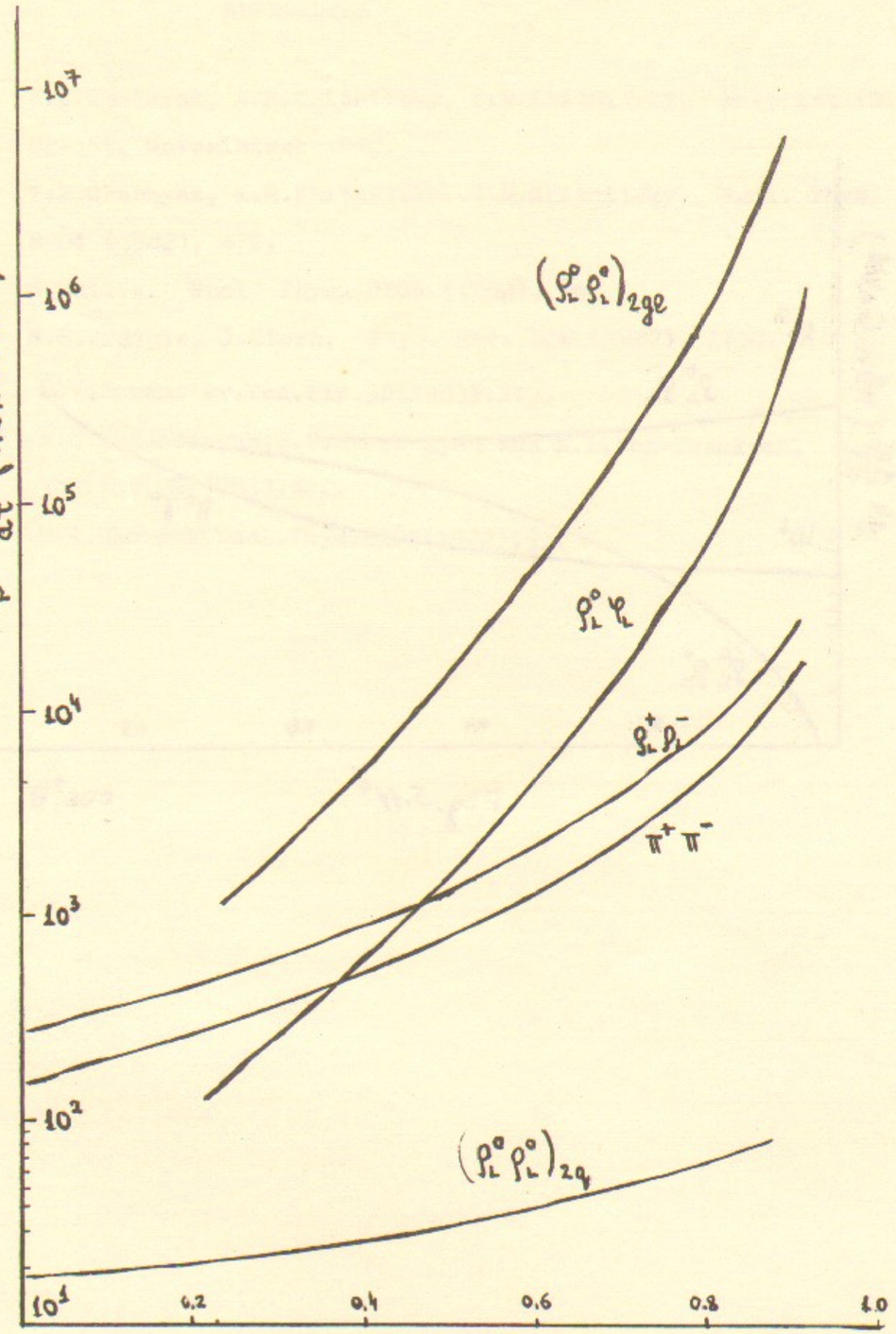


Fig. 5.11

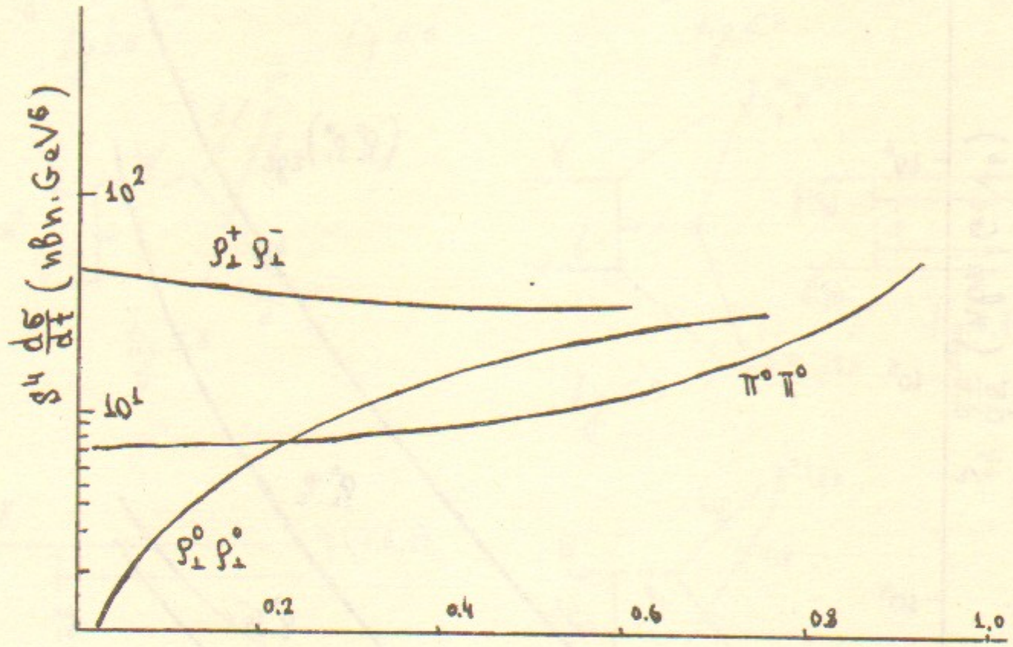


Fig. 5.11[6]



REFERENCES


4.1 V.L.Chernyak, A.R.Zhitnitsky, I.R.Zhitnitsky, Preprint INP 82-159, Novosibirsk 1982.

4.2 V.L.Chernyak, A.R.Zhitnitsky, I.R.Zhitnitsky, Nucl. Phys. B204 (1982), 477.

4.3 S.Mallik, Nucl. Phys. B206 (1982), 90.

4.4 N.S.Craigie, J.Stern, Phys. Rev. D26 (1982), 2430.

4.5[a] M.V.Terent'ev, Yad.Fiz.38(1983),213.

4.5[b] A.S.Bagdasaryan, S.V.Esaybegyan and N.L.ter-Isaakyan, Yad.Fiz.38(1983),402.

4.6 E.V.Shuryak.Nucl.Phys.B203(1982),93.

REFERENCES


5.1 V.A.Novikov e.a., Nucl. Phys. B191 (1981), 301.

5.2 J.Ellis, M.K.Gaillard, D.V.Nanopoulos, Nucl. Phys. B100 (1975), 313.
M.K.Gaillard, B.W.Lee, J.L.Rosner, Rev. Mod. Phys. 47 (1975), 277.

5.3 D.Fakirov and B.Stech, Nucl.Phys. B133(1978)315

5.4 M.Bander, D.Silverman, A.Soni, Phys. Rev. Lett. 44 (1980)7

H.Fritzsch, P.Minkovski, Phys. Lett. 90B (1980), 455.
W.Bernreuther, O.Nachtmann, B.Stech, Z. Phys. C4 (1980), 257.

5.5 a) H.J.Lipkin, Phys. Rev. Lett 44 (1980), 710.
b) B.Guberina, S.Nussinov, R.D.Peccei, R.Ruckl, Phys. Lett 89B (1979), 111.
V.Barger, J.P.Leveille, P.M.Stevenson, Phys. Rev. Lett 44 (1980), 226.
S.P.Rosen, Phys. Rev. Lett. 44(1980), 4.
I.I.Bigi, Z. Phys. C5 (1980), 313.
Q.Ho-Kim, H.C.Lee, Phys. Lett. 100B (1981), 420.
C.J.Gilmour, preprint 82/28 DAMTP.

5.6 G.Trilling, Phys. Rep. v. 75 (1981), 57.

5.7 H.Fritzch, Preprint MPI-PAE/pth 51/80 (November 1980).
R.D.Peccei, Preprint MPI-PAE/pth 6/80 (April 1980).
R.Ruckl, Preprint MPI-PAE/pth 23/80 (July 1980)

5.8 L.Maiani, Talk at the XXI Int. Conf. on High Energy Physics, Paris, 1982.

5.9 M.K.Gaillard, B.W.Lee, Phys. Rev. Lett. 33(1974), 108.
G.Altarelli, L.Maiani, Phys. Lett. 52B (1974), 351.





5.10 A.I.Vainshtein, V.I.Zakharov, M.A.Shifman, JETP (Sov. Phys.) 45 (1977), 670.

5.11 A.K.Honma, SLAC report-295 (1980).

5.12 B.Hyams et al., Nucl. Phys. B100 (1975), 205.
P.Estabrooks, A.D.Martin, Nucl. Phys. B95 (1975), 322.
P.Estabrooks et al., Nucl. Phys. B133 (1978), 490.

5.13 4-th Intern. Colloq. on Photon-photon Interactions, Paris, April 1981.

5.14 V.E.Balakin, G.I.Budker, A.N.Skrinsky, Preprint INP-78--101, Novosibirsk 1978.
V.E.Balakin, A.N.Skrinsky, "VLEPP Project (Status report)" Preprint INP-81-129, Novosibirsk, 1981.

5.15 SLAC Report 229, 1980.
B.Richter et al., Preprint SLAC-PUB-2549, 1980
P.Panofsky, Report at Intern, Symp. on Lepton and Photon Interactions at High Energies, Bonn, 1981.

5.16 I.F.Ginzburg, G.L.Kotkin, V.G.Serbo, V.I.Telnov, Pis'ma v Zh. Eksp. Teor. Fiz. 9 (1981), 514.

5.17 S.J.Brodsky, G.P.Lepage, Phys. Rev. D24 (1981), 1808.

5.18 V.L.Chernyak, I.R.Zhitnitsky, Nucl. Phys. B222(1983), 406

5.19 See P.V.Landshoff in 5.13 .

5.20 H.Cheng, T.T.Wu, Phys. Rev. D1(1970), 3414.
L.N.Lipatov, G.V.Frolov, Yad. Fiz. 13 (1971), 333.

5.21 P.H. Damgaard, Nucl. Phys. B211(1983)435

5.22 K.G.Königsmann, Preprint SLAC-PUB-2910,Stanford,1982

А.Р.Житницкий, В.Л.Черняк

# АСИМПТОТИЧЕСКОЕ ПОВЕДЕНИЕ ЭКСКЛЮЗИВНЫХ ПРОЦЕССОВ В КХД

4. Волновые функции ведущего твиста $\pi$ , $\rho$ - мезонов и правила сумм КХД
5. Применения. Расчеты конкретных процессов.

Препринт
№ 83-105

Работа поступила - 28 июня 1983 г.

Ответственный за выпуск - С.Г.Попов
Подписано к печати 15.07-1983 г. МН 17643
Формат бумаги 60x90 1/16 Усл.3,0 печ.л., 2,4 учетно-изд.л.
Тираж 290 экз. Бесплатно. Заказ № 105.

Ротапринт ИЯФ СО АН СССР, г.Новосибирск, 90